KA-TP-12-1997

Electroweak Radiative Corrections after the Top Quark Discovery

W. Hollik
Institut für Theoretische Physik
Universität Karlsruhe
D-76128 Karlsruhe, Germany

to appear in: Second Edition of "Heavy Flavors",
edited by A.J. Buras and M. Lindner,
World Scientific, Singapore

Electroweak Radiative Corrections after the Top Quark Discovery

Wolfgang Hollik
Institut für Theoretische Physik
Universität Karlsruhe
D-76128 Karlsruhe, Germany

In this article we give a discussion of the structure of the electroweak Standard Model and its quantum corrections for tests of the electroweak theory. The predictions for the vector boson masses and the Z resonance observables are presented in some detail. We show comparisons with the recent experimental data and their implications for the present status of the Standard Model. Finally we address the question how virtual New Physics can influence the predictions for the precision observables and discuss the minimal supersymmetric standard model as a special example of particular theoretical interest.

1 Introduction

The present theory of the electroweak interaction, known as the "Standard Model" [1,2,3,4] is a gauge invariant quantum field theory with the symmetry group SU(2)×U(1) spontaneously broken by the Higgs mechanism. It contains essentially three free parameters to describe the gauge bosons $\gamma, W^{\pm}, Z$ and their interactions with the fermions. For a comparison between theory and experiment three independent experimental input data are required. The most natural choice is given by the electromagnetic fine structure constant α, the muon decay constant (Fermi constant) G_μ, and the mass of the Z boson which has meanwhile been measured with the same accuracy as G_μ. Other measurable quantities are predicted in terms of the input data. Each additional precision experiment which allows the detection of small deviations from the lowest order predictions can be considered a test of the electroweak theory at the quantum level. In the Feynman graph expansion of the scattering amplitude for a given process the higher order terms show up as diagrams containing closed loops. The lowest order amplitudes could also be derived from a corresponding classical field theory whereas the loop contributions can only be obtained from the quantized version. The renormalizability of the Standard Model [5] ensures that it retains its predictive power also in higher orders. The higher order terms, commonly called radiative corrections, are the quantum effects of the electroweak theory. They are complicated in their concrete form, but they are finally the consequence of the basic Lagrangian with a simple structure. The quantum corrections contain the self-coupling of the vector bosons as well as their interactions with the Higgs field and the top quark, and provide the theoretical basis for electroweak precision tests. Assuming

the validity of the Standard model, the presence of the top quark and the Higgs boson in the loop contributions to electroweak observables allows to obtain significant bounds on their masses from precision measurements of these observables.

The present generation of high precision experiments hence imposes stringent tests on the Standard Model. Besides the impressive achievements in the determination of the Z boson parameters [6] and the W mass [7,6], the most important step has been the discovery of the top quark at the Tevatron [8] with the mass determination $m_t = 175.6 \pm 5.5$ GeV, which coincides perfectly with the indirectly obtained mass range via the radiative corrections. Moreover, with the top mass as an additional precise experimental data point one now can fully exploit the sensitivity to the Higgs mass.

The high experimental sensitivity in the electroweak observables, at the level of the quantum effects, requires the highest standards on the theoretical side as well. A sizeable amount of work has contributed over the last few years to a steadily rising improvement of the standard model predictions pinning down the theoretical uncertainties to a level sufficiently small for the current interpretation of the precision data, but still sizeable enough to provoke conflict with a further increase in the experimental accuracy.

The lack of direct signals from "New Physics" makes the high precision experiments also a unique tool in the search for *indirect* effects: through definite deviations of the experimental results from the theoretical predictions of the minimal Standard Model. Since such deviations are expected to be small, of the typical size of the Standard Model radiative corrections, it is inevitable to have the the standard loop effects in the precision observables under control.

In this article we give a brief discussion of the structure of the Standard Model and its quantum corrections for testing the electroweak theory at present and future colliders. The predictions for the vector boson masses, neutrino scattering cross sections, and the Z resonance observables like the width of the Z resonance, partial widths, effective neutral current coupling constants and mixing angles at the Z peak, are presented in some detail. We show comparisons with the recent experimental data and their implications for the present status of the Standard Model. Finally we address the question how virtual New Physics can influence the predictions for the precision observables and discuss the minimal supersymmetric standard model (MSSM) as a special example of particular theoretical interest.

2 The electroweak Standard Model

2.1 The Standard Model Lagrangian

The phenomenological basis for the formulation of the Standard Model is given by the following empirical facts:

- The SU(2)×U(1) family structure of the fermions:
  The fermions appear as families with left-handed doublets and right-handed singlets:

$$\begin{pmatrix} \nu_e \\ e \end{pmatrix}_L, \quad \begin{pmatrix} \nu_\mu \\ \mu \end{pmatrix}_L, \quad \begin{pmatrix} \nu_\tau \\ \tau \end{pmatrix}_L, \quad e_R, \quad \mu_R, \quad \tau_R$$

$$\begin{pmatrix} u \\ d \end{pmatrix}_L, \quad \begin{pmatrix} c \\ s \end{pmatrix}_L, \quad \begin{pmatrix} t \\ b \end{pmatrix}_L, \quad u_R, \quad d_R, \quad c_R, \cdots$$

  They can be characterized by the quantum numbers of the weak isospin I, I_3, and the weak hypercharge Y.

- The Gell-Mann-Nishijima relation:
  Between the quantum numbers classifying the fermions with respect to the group SU(2)×U(1) and their electric charges Q the relation

$$Q = I_3 + \frac{Y}{2} \tag{1}$$

  is valid.

- The existence of vector bosons:
  There are 4 vector bosons as carriers of the electroweak force

$$\gamma, \quad W^+, \quad W^-, \quad Z$$

  where the photon is massless and the $W^\pm$, Z have masses $M_W \neq 0$, $M_Z \neq 0$.

This empirical structure can be embedded in a gauge invariant field theory of the unified electromagnetic and weak interactions by interpreting SU(2)×U(1) as the group of gauge transformations under which the Lagrangian is invariant. This full symmetry has to be broken by the Higgs mechanism down to the electromagnetic gauge symmetry; otherwise the $W^\pm$, Z bosons would also be massless. The minimal formulation, the Standard Model, requires a single scalar field (Higgs field) which is a doublet under SU(2).

According to the general principles of constructing a gauge invariant field theory with spontaneous symmetry breaking, the gauge, Higgs, and fermion parts of the electroweak Lagrangian

$$\mathcal{L}_{cl} = \mathcal{L}_G + \mathcal{L}_H + \mathcal{L}_F \tag{2}$$

are specified in the following way:

Gauge fields
SU(2)×U(1) is a non-Abelian group which is generated by the isospin operators I_1, I_2, I_3 and the hypercharge Y (the elements of the corresponding Lie algebra). Each of these generalized charges is associated with a vector field: a triplet of vector fields $W_\mu^{1,2,3}$ with $I_{1,2,3}$ and a singlet field B_μ with Y. The isotriplet W_μ^a, $a = 1, 2, 3$, and the isosinglet B_μ lead to the field strength tensors

$$\begin{aligned} W_{\mu\nu}^a &= \partial_\mu W_\nu^a - \partial_\nu W_\mu^a + g_2\, \epsilon_{abc}\, W_\mu^b W_\nu^c, \\ B_{\mu\nu} &= \partial_\mu B_\nu - \partial_\nu B_\mu. \end{aligned} \tag{3}$$

g_2 denotes the non-Abelian SU(2) gauge coupling constant and g_1 the Abelian U(1) coupling. From the field tensors (3) the pure gauge field Lagrangian

$$\mathcal{L}_G = -\frac{1}{4}\, W_{\mu\nu}^a W^{\mu\nu,a} - \frac{1}{4}\, B_{\mu\nu} B^{\mu\nu} \tag{4}$$

is formed according to the rules for the non-Abelian case.

Fermion fields and fermion-gauge interaction
The left-handed fermion fields of each lepton and quark family (colour index is suppressed)

$$\psi_j^L = \begin{pmatrix} \psi_{j+}^L \\ \psi_{j-}^L \end{pmatrix}$$

with family index j are grouped into SU(2) doublets with component index $\sigma = \pm$, and the right-handed fields into singlets

$$\psi_j^R = \psi_{j\sigma}^R.$$

Each left- and right-handed multiplet is an eigenstate of the weak hypercharge Y such that the relation (1) is fulfilled. The covariant derivative

$$D_\mu = \partial_\mu - i\, g_2\, I_a W_\mu^a + i\, g_1\, \frac{Y}{2}\, B_\mu \tag{5}$$

induces the fermion-gauge field interaction via the minimal substitution rule:

$$\mathcal{L}_F = \sum_j \bar{\psi}_j^L i\gamma^\mu D_\mu \psi_j^L + \sum_{j,\sigma} \bar{\psi}_{j\sigma}^R i\gamma^\mu D_\mu \psi_{j\sigma}^R \tag{6}$$

Higgs field, Higgs - gauge field and Yukawa interaction
For spontaneous breaking of the SU(2)×U(1) symmetry leaving the electromagnetic gauge subgroup $U(1)_{em}$ unbroken, a single complex scalar doublet field with hypercharge $Y = 1$

$$\Phi(x) = \begin{pmatrix} \phi^+(x) \\ \phi^0(x) \end{pmatrix} \tag{7}$$

is coupled to the gauge fields

$$\mathcal{L}_H = (D_\mu \Phi)^+ (D^\mu \Phi) - V(\Phi) \tag{8}$$

with the covariant derivative

$$D_\mu = \partial_\mu - i\, g_2\, I_a W_\mu^a + i\, \frac{g_1}{2}\, B_\mu \,.$$

The Higgs field self-interaction

$$V(\Phi) = -\mu^2\, \Phi^+ \Phi + \frac{\lambda}{4}\, (\Phi^+ \Phi)^2 \tag{9}$$

is constructed in such a way that it has a non-vanishing vacuum expectation value v, related to the coefficients of the potential V by

$$v = \frac{2\mu}{\sqrt{\lambda}} \,. \tag{10}$$

The field (7) can be written in the following way:

$$\Phi(x) = \begin{pmatrix} \phi^+(x) \\ (v + H(x) + i\chi(x))/\sqrt{2} \end{pmatrix} \tag{11}$$

where the components ϕ^+, H, χ now have vacuum expectation values zero. Exploiting the invariance of the Lagrangian one notices that the components ϕ^+, χ can be gauged away which means that they are unphysical (Higgs ghosts or would-be Goldstone bosons). In this particular gauge, the unitary gauge, the Higgs field has the simple form

$$\Phi(x) = \frac{1}{\sqrt{2}} \begin{pmatrix} 0 \\ v + H(x) \end{pmatrix} \,.$$

The real part of ϕ^0, $H(x)$, describes physical neutral scalar particles with mass

$$M_H = \mu\sqrt{2}. \tag{12}$$

The Higgs field components have triple and quartic self couplings following from V, and couplings to the gauge fields via the kinetic term of Eq. (8).

In addition, Yukawa couplings to fermions are introduced in order to make the charged fermions massive. The Yukawa term is conveniently expressed in the doublet field components (7). We write it down for one family of leptons and quarks:

$$\begin{aligned} \mathcal{L}_{Yukawa} &= -g_l\,(\overline{\nu}_L\,\phi^+\,l_R \,+\, \overline{l}_R\,\phi^-\,\nu_L \,+\, \overline{l}_L\,\phi^0\,l_R \,+\, \overline{l}_R\,\phi^{0*}\,l_L) \\ &= -g_d\,(\overline{u}_L\,\phi^+\,d_R \,+\, \overline{d}_R\,\phi^-\,u_L \,+\, \overline{d}_L\,\phi^0\,d_R \,+\, \overline{d}_R\,\phi^{0*}\,d_L) \\ &\quad -g_u\,(-\overline{u}_R\,\phi^+\,d_L \,-\, \overline{d}_L\,\phi^-\,u_R \,+\, \overline{u}_R\,\phi^0\,u_L \,+\, \overline{u}_L\,\phi^{0*}\,u_R)\,. \end{aligned} \tag{13}$$

ϕ^- denotes the adjoint of ϕ^+.

By $v \neq 0$ fermion mass terms are induced. The Yukawa coupling constants $g_{l,d,u}$ are related to the masses of the charged fermions by Eq. (23). In the unitary gauge the Yukawa Lagrangian is particularly simple:

$$\mathcal{L}_{Yukawa} \;=\; -\sum_f m_f\;\bar{\psi}_f\psi_f - \sum_f \frac{m_f}{v}\;\bar{\psi}_f\psi_f\;H\,. \tag{14}$$

As a remnant of this mechanism for generating fermion masses in a gauge invariant way, Yukawa interactions between the massive fermions and the physical Higgs field occur with coupling constants proportional to the fermion masses.

Physical fields and parameters

The gauge invariant Higgs-gauge field interaction in the kinetic part of Eq. (8) gives rise to mass terms for the vector bosons in the non-diagonal form

$$\frac{1}{2}\left(\frac{g_2}{2}v\right)^2\,(W_1^2+W_2^2) + \frac{v^2}{4}\,(W_\mu^3, B_\mu)\begin{pmatrix} g_2^2 & g_1g_2 \\ g_1g_2 & g_1^2 \end{pmatrix}\begin{pmatrix} W_\mu^3 \\ B_\mu \end{pmatrix}\,. \tag{15}$$

The physical content becomes transparent by performing a transformation from the fields W_μ^a, B_μ (in terms of which the symmetry is manifest) to the "physical" fields

$$W_\mu^\pm = \frac{1}{\sqrt{2}}\,(W_\mu^1 \pm iW_\mu^2) \tag{16}$$

and

$$\begin{aligned} Z_\mu &= +\cos\theta_W\, W^3_\mu + \sin\theta_W\, B_\mu \\ A_\mu &= -\sin\theta_W\, W^3_\mu + \cos\theta_W\, B_\mu \end{aligned} \tag{17}$$

In these fields the mass term (15) is diagonal and has the form

$$M_W^2\, W^+_\mu W^{-\mu} + \frac{1}{2}\,(A_\mu, Z_\mu) \begin{pmatrix} 0 & 0 \\ 0 & M_Z^2 \end{pmatrix} \begin{pmatrix} A^\mu \\ Z^\mu \end{pmatrix} \tag{18}$$

with

$$\begin{aligned} M_W &= \frac{1}{2}\, g_2 v \\ M_Z &= \frac{1}{2}\sqrt{g_1^2 + g_2^2}\, v \end{aligned} \tag{19}$$

The mixing angle in the rotation (17) is given by

$$\cos\theta_W = \frac{g_2}{\sqrt{g_1^2 + g_2^2}} = \frac{M_W}{M_Z}\,. \tag{20}$$

Identifying A_μ with the photon field which couples via the electric charge $e = \sqrt{4\pi\alpha}$ to the electron, e can be expressed in terms of the gauge couplings in the following way

$$e = \frac{g_1 g_2}{\sqrt{g_1^2 + g_2^2}} \tag{21}$$

or

$$g_2 = \frac{e}{\sin\theta_W}, \quad g_1 = \frac{e}{\cos\theta_W}. \tag{22}$$

Finally, from the Yukawa coupling terms in Eq. (13) the fermion masses are obtained:

$$m_f = g_f\, \frac{v}{\sqrt{2}} = \sqrt{2}\, \frac{g_f}{g_2}\, M_W\,. \tag{23}$$

The relations above allow one to replace the original set of parameters

$$g_2,\ g_1,\ \lambda,\ \mu^2,\ g_f \tag{24}$$

by the equivalent set of more physical parameters

$$e,\ M_W,\ M_Z,\ M_H,\ m_f \tag{25}$$

where each of them can (in principle) directly be measured in a suitable experiment.

An additional very precisely measured parameter is the Fermi constant G_μ which is the effective 4-fermion coupling constant in the the Fermi model, measured by the muon lifetime:

$$G_\mu = 1.16639(2) \cdot 10^{-5}\,\mathrm{GeV}^{-2}$$

Consistency of the Standard Model at $q^2 \ll M_W^2$ with the Fermi model requires the identification (see section 4)

$$\frac{G_\mu}{\sqrt{2}} = \frac{e^2}{8 \sin^2\theta_W M_W^2}\,, \tag{26}$$

which allows us to relate the vector boson masses to the parameters α, G_μ, and $\sin^2\theta_W$ as follows:

$$\begin{aligned} M_W^2 &= \frac{\pi\alpha}{\sqrt{2}G_\mu} \cdot \frac{1}{\sin^2\theta_W} \\ M_Z^2 &= \frac{\pi\alpha}{\sqrt{2}G_\mu} \cdot \frac{1}{\sin^2\theta_W \cos^2\theta_W} \end{aligned} \tag{27}$$

and thus to establish also the $M_W - M_Z$ interdependence:

$$M_W^2 \left(1 - \frac{M_W^2}{M_Z^2}\right) = \frac{\pi\alpha}{\sqrt{2}G_\mu}\,. \tag{28}$$

2.2 Gauge fixing and ghost fields

Since the S matrix element for any physical process is a gauge invariant quantity it is possible to work in the unitary gauge with no unphysical particles in internal lines. For a systematic treatment of the quantization of $\mathcal{L}_{cl}$ and for higher order calculations, however, one better refers to a renormalizable gauge. This can be done by adding to $\mathcal{L}_{cl}$ a gauge fixing Lagrangian, for example

$$\mathcal{L}_{fix} = -\frac{1}{2}\left(F_\gamma^2 + F_Z^2 + 2F_+F_-\right) \tag{29}$$

with linear gauge fixings of the 't Hooft type:

$$\begin{aligned} F_\pm &= \frac{1}{\sqrt{\xi^W}}\left(\partial^\mu W_\mu^\pm \mp i M_W \xi^W \phi^\pm\right) \\ F_Z &= \frac{1}{\sqrt{\xi^Z}}\left(\partial^\mu Z_\mu - M_Z \xi^Z \chi\right) \\ F_\gamma &= \frac{1}{\sqrt{\xi^\gamma}}\,\partial^\mu A_\mu \end{aligned} \tag{30}$$

with arbitrary parameters $\xi^{W,Z,\gamma}$. In this class of 't Hooft gauges, the vector boson propagators have the form

$$\frac{i}{k^2 - M_V^2}\left(-g^{\mu\nu} + \frac{(1-\xi^V)k^\mu k^\nu}{k^2 - \xi^V M_V^2}\right)$$

$$= \frac{i}{k^2 - M_V^2}\left(-g^{\mu\nu} + \frac{k^\mu k^\nu}{k^2}\right) + \frac{i\xi^V}{k^2 - \xi^V M_V^2}\frac{k^\mu k^\nu}{k^2}, \tag{31}$$

the propagators for the unphysical Higgs fields are given by

$$\frac{i}{k^2 - \xi^W M_W^2} \quad \text{for} \quad \phi^\pm \tag{32}$$

$$\frac{i}{k^2 - \xi^Z M_Z^2} \quad \text{for} \quad \chi^0\,, \tag{33}$$

and Higgs-vector boson transitions do not occur.

For completion of the renormalizable Lagrangian the Faddeev-Popov ghost term $\mathcal{L}_{gh}$ has to be added [9] in order to balance the undesired effects in the unphysical components introduced by $\mathcal{L}_{fix}$:

$$\mathcal{L} = \mathcal{L}_{cl} + \mathcal{L}_{fix} + \mathcal{L}_{gh} \tag{34}$$

where

$$\mathcal{L}_{gh} = \bar{u}^\alpha(x)\frac{\delta F^\alpha}{\delta\theta^\beta(x)}u^\beta(x) \tag{35}$$

with ghost fields u^γ, u^Z, $u^\pm$, and $\frac{\delta F^\alpha}{\delta\theta^\beta}$ being the change of the gauge fixing operators (30) under infinitesimal gauge transformations characterized by $\theta^\alpha(x) = \{\theta^a(x),\, \theta^Y(x)\}$.

In the 't Hooft-Feynman gauge ($\xi = 1$) the vector boson propagators (31) become particularly simple: the transverse and longitudinal components, as well as the propagators for the unphysical Higgs fields $\phi^\pm$, χ and the ghost fields $u^\pm$, u^Z have poles which coincide with the masses of the corresponding physical particles $W^\pm$ and Z.

2.3 Feynman rules

Expressed in terms of the physical parameters we can write down the Lagrangian

$$\mathcal{L}(A_\mu, W_\mu^\pm, Z_\mu, H, \phi^\pm, \chi, u^\pm, u^Z, u^\gamma;\, M_W, M_Z, e, \ldots)$$

in a way which allows us to read off the propagators and the vertices most directly. We specify them in the $R_{\xi=1}$ gauge where the vector boson propagators have the simple algebraic form $\sim g_{\mu\nu}$.

$$\mathcal{L}_G + \mathcal{L}_H \;=$$

$$\begin{aligned}
\frac{1}{2} A_\mu \,\Box\, A^\mu \qquad &\leftrightarrow \qquad \frac{-i\, g_{\mu\nu}}{q^2} \\
+ W^-_\mu \,(\Box + M_W^2)\, W^{+\mu} \qquad &\leftrightarrow \qquad \frac{-i\, g_{\mu\nu}}{q^2 - M_W^2} \\
+ \frac{1}{2} Z_\mu \,(\Box + M_Z^2)\, Z^\mu \qquad &\leftrightarrow \qquad \frac{-i\, g_{\mu\nu}}{q^2 - M_Z^2} \\
+ \frac{1}{2} H \,(\Box + M_H^2)\, H \qquad &\leftrightarrow \qquad \frac{i}{q^2 - M_H^2}
\end{aligned}$$

$$\begin{aligned}
&+ \text{interaction terms} \\
&\quad VV,\; VH,\; HH
\end{aligned}$$

$$+ \text{(unphysical degrees of freedom)}$$

$$\mathcal{L}_F + \mathcal{L}_{Yukawa} \;=$$

$$\begin{aligned}
\sum_f \bar{f}\,(i\partial - m_f)\, f \qquad &\leftrightarrow \qquad \frac{i}{\not{q} - m_f} \\
+ J^\mu_{em}\, A_\mu \qquad &\leftrightarrow \qquad -i\, e\, Q_f \gamma_\mu \\
+ J^\mu_{NC}\, Z_\mu \qquad &\leftrightarrow \qquad i\, \frac{e}{2 \sin\theta_W \cos\theta_W}\, \gamma_\mu (v_f - a_f \gamma_5) \\
+ J^\mu_{CC}\, W_\mu \qquad &\leftrightarrow \qquad i\, \frac{e}{2\sqrt{2} \sin\theta_W}\, \gamma_\mu (1 - \gamma_5)\, V_{jk}
\end{aligned}$$

$$-\frac{g_f}{\sqrt{2}}\,\bar{f}f\,H \qquad \leftrightarrow \qquad -i\,\frac{g_f}{\sqrt{2}} = i\,\frac{e}{2\sin\theta_W}\,\frac{m_f}{M_W}$$

$+$ (unphysical degrees of freedom) (36)

These Feynman rules provide the ingredients to calculate the lowest order amplitudes for fermionic processes. For the complete list of all interaction vertices we refer to the literature [10].

In order to describe scattering processes between light fermions in lowest order we can, in most cases, neglect the exchange of Higgs bosons because of their small Yukawa couplings to the light fermions. The standard processes accessible by the experimental facilities are basically 4-fermion processes. These are mediated by the gauge bosons and, sufficient in lowest order, defined by the vertices for the fermions interacting with the vector bosons. They are given in the Lagrangian above for the electromagnetic, neutral and charged current interactions. The neutral current coupling constants in (36) read

$$\begin{aligned} v_f &= I_3^f - 2Q_f \sin^2\theta_W \\ a_f &= I_3^f\,. \end{aligned} \tag{37}$$

Q_f and I_3^f denote the charge and the third isospin component of f_L.

The quantities V_{jk} in the charged current vertex are the elements of the unitary 3×3 matrix

$$U_{KM} = \begin{pmatrix} V_{ud} & V_{us} & V_{ub} \\ V_{cd} & V_{cs} & V_{cb} \\ V_{td} & V_{ts} & V_{tb} \end{pmatrix} \tag{38}$$

which describes family mixing in the quark sector [3]. Its origin is the diagonalization of the quark mass matrices from the Yukawa coupling which appears since quarks of the same charge have different masses. For massless neutrinos no mixing in the leptonic sector is present. Due to the unitarity of U_{KM} the mixing is absent in the neutral current.

For a proper treatment of the charged current vertex at the one-loop level, the matrix U_{KM} has to be renormalized as well. As it was shown in [11], where the renormalization procedure was extended to U_{KM}, the resulting effects are completely negligible for the known light fermions. We therefore skip the renormalization of U_{KM} in our discussion of radiative corrections.

3 Renormalization

3.1 General remarks

In higher order perturbation theory the relations between the formal parameters and measureable quantities are different from the tree level relations in general. Moreover, the procedure is obscured by the appearence of divergences from the loop integrations. For a mathematically consistent treatment one has to regularize the theory, e.g. by dimensional regularization (performing the calculations in D dimensions). But then the relations between physical quantities and the parameters become cutoff dependent. Hence, the parameters of the basic Lagrangian, the "bare" parameters, have no physical meaning. On the other hand, relations between measureable physical quantities, where the parameters drop out, are finite and independent of the cutoff. It is therefore in principle possible to perform tests of the theory in terms of such relations by eliminating the bare parameters [12,13].

Alternatively, one may replace the bare parameters by renormalized ones by multiplicative renormalization for each bare parameter g_0

$$g_0 = Z_g\, g = g + \delta g \tag{39}$$

with renormalization constants Z_g different from 1 by a 1-loop term. The renormalized parameters g are finite and fixed by a set of renormalization conditions. The decomposition (39) is to a large extent arbitrary. Only the divergent parts are determined directly by the structure of the divergences of the one-loop amplitudes. The finite parts depend on the choice of the explicit renormalization conditions.

The simplest way to obtain a set of finite Green functions is the "minimal subtraction scheme" [14] where (in dimensional regularization) the singular part of each divergent diagram is subtracted and the parameters are defined at an arbitrary mass scale μ. This scheme, with slight modifications, has been applied in QCD where due to the confinement of quarks and gluons there is no distinguished mass scale in the renormalization procedure.

The situation is different in QED and in the electroweak theory. There the classical Thomson scattering and the particle masses set natural scales where the parameters can be defined. In QED the favoured renormalization scheme is the on-shell scheme where $e = \sqrt{4\pi\alpha}$ and the electron, muon, ... masses are used as input parameters. The finite parts of the counter terms are fixed by the renormalization conditions that the fermion propagators have poles at their physical masses, and e becomes the $ee\gamma$ coupling constant in the Thomson limit

of Compton scattering. In the electroweak Standard Model a distinguished set for parameter renormalization is given in terms of e, M_Z, M_W, M_H, m_f with the masses of the corresponding particles. This electroweak on-shell scheme is the straight-forward extension of the familiar QED renormalization, first proposed by Ross and Taylor [15] and used in many practical applications [10,16,17,18,19,20,21,22,23,24,25]. The mass of the Higgs boson, as long as it is experimentally unknown, is treated as a free input parameter. The light quark masses can only be considered as effective parameters. In the cases of practical interest they can be replaced in terms of directly measured quantities like the cross section for $e^+e^- \to$ hadrons.

The electroweak mixing angle is related to the vector boson masses in general by

$$\sin^2\theta_W \;=\; 1 - \frac{M_W^2}{\rho_0\, M_Z^2} \tag{40}$$

where $\rho_0 \neq 1$ at the tree level in case of a Higgs system more complicated than with doublets only. We want to restrict our discussion of radiative corrections primarily to the minimal model with $\rho_0 = 1$. For $\rho \neq 1$ see section 7.1.

Instead of the set e, M_W, M_Z as basic free parameters one may alternatively use as basic parameters α, G_μ, M_Z [26] or α, G_μ, $\sin^2\theta_W$ with the mixing angle deduced from neutrino-electron scattering [27] or perform the loop calculations in the $\overline{MS}$ scheme [28,29,30,31]. The so-called $*$-scheme [32,33] is a different way of book-keeping in terms of effective running couplings. Here we follow the line of the on-shell scheme as specified in detail in [10,24], but skip field renormalization.

3.2 Mass renormalization

We have now to discuss the 1-loop contributions to the on-shell parameters and their renormalization. Since the boson masses are part of the propagators we have to investigate the effects of the W and Z self-energies.

We restrict our discussion to the transverse parts $\sim g_{\mu\nu}$. In the electroweak theory, differently from QED, the longitudinal components $\sim q_\mu q_\nu$ of the vector boson propagators do not give zero results in physical matrix elements. But for light external fermions the contributions are suppressed by $(m_f/M_Z)^2$ and we are allowed to neglect them. Writing the self-energies as

$$\Sigma^{W,Z}_{\mu\nu} = g_{\mu\nu}\Sigma^{W,Z} + \cdots \tag{41}$$

with scalar functions $\Sigma^{W,Z}(q^2)$ we have for the 1-loop propagators ($V = W, Z$)

$$\frac{-ig^{\mu\sigma}}{q^2 - M_V^2} \left(-i\,\Sigma^V_{\rho\sigma}\right) \frac{-ig^{\rho\nu}}{q^2 - M_V^2} = \frac{-ig^{\mu\nu}}{q^2 - M_V^2} \left(\frac{-\Sigma^V(q^2)}{q^2 - M_V^2}\right) \tag{42}$$

(the factor $-i$ in the self energy insertion is a convention). Besides the fermion loop contributions in the electroweak theory there are also the non-Abelian gauge boson loops and loops involving the Higgs boson. The Higgs boson thus enters the 4-fermion amplitudes as an experimentally unknown object at the level of radiative corrections with its mass to be treated as an additional free parameter. In the graphical representation, the self-energies for the vector bosons denote the sum of all the diagrams with virtual fermions, vector bosons, Higgs and ghost loops.

Resumming all self energy-insertions yields a geometrical series for the dressed propagators:

$$\begin{aligned} &\frac{-ig_{\mu\nu}}{q^2 - M_V^2} \left[1 + \left(\frac{-\Sigma^V}{q^2 - M_V^2}\right) + \left(\frac{-\Sigma^V}{q^2 - M_V^2}\right)^2 + \cdots\right] \\ &= \frac{-ig_{\mu\nu}}{q^2 - M_V^2 + \Sigma^V(q^2)}\,. \end{aligned} \tag{43}$$

The locations of the poles in the propagators are shifted by the self-energies. Consequently, the principal step in *mass renormalization* consists in a re-interpretation of the parameters: the masses in the Lagrangian cannot be the physical masses of W and Z but are the "bare masses" related to the physical masses M_W, M_Z by

$$\begin{aligned} M_W^{0\,2} &= M_W^2 + \delta M_W^2 \\ M_Z^{0\,2} &= M_Z^2 + \delta M_Z^2 \end{aligned} \tag{44}$$

with counterterms of 1-loop order. The "correct" propagators according to this prescription are given by

$$\frac{-ig_{\mu\nu}}{q^2 - M_V^{0\,2} + \Sigma^V(q^2)} = \frac{-ig_{\mu\nu}}{q^2 - M_V^2 - \delta M_V^2 + \Sigma^V(q^2)}\,. \tag{45}$$

instead of Eq. (45). The renormalization conditions which ensure that $M_{W,Z}$ are the physical masses fix the mass counterterms to be

$$\begin{aligned} \delta M_W^2 &= \mathrm{Re}\,\Sigma^W(M_W^2) \\ \delta M_Z^2 &= \mathrm{Re}\,\Sigma^Z(M_Z^2)\,. \end{aligned} \tag{46}$$

In this way, two of our input parameters and their counterterms have been defined.

3.3 Charge renormalization

Our third input parameter is the electromagnetic charge e. The electroweak *charge renormalization* is very similar to that in pure QED. As in QED, we want to maintain the definition of e as the classical charge in the Thomson cross section

$$\sigma_{Th} = \frac{e^4}{6\pi\, m_e^2}\,.$$

Accordingly, the Lagrangian carries the bare charge $e_0 = e + \delta e$ with the charge counter term δe of 1-loop order. The charge counter term δe has to absorb the electroweak loop contributions to the $ee\gamma$ vertex in the Thomson limit. This charge renormalization condition is simplified by the validity of a generalization of the QED Ward identity[34] which implies that those corrections related to the external particles cancel each other. Thus for δe only two universal contributions are left [we use $s_W = \sin\theta_W$, $c_W = \cos\theta_W$ as abbreviations]:

$$\frac{\delta e}{e} = \frac{1}{2}\,\Pi^\gamma(0) - \frac{s_W}{c_W}\,\frac{\Sigma^{\gamma Z}(0)}{M_Z^2}\,. \tag{47}$$

The first one, quite in analogy to QED, is given by the vacuum polarization of the photon. But now, besides the fermion loops, it contains also bosonic loop diagrams from W^+W^- virtual states and the corresponding ghosts. The second term contains the mixing between photon and Z, in general described as a mixing propagator with $\Sigma^{\gamma Z}$ normalized as

$$\Delta^{\gamma Z} = \frac{-ig_{\mu\nu}}{q^2}\left(\frac{-\Sigma^{\gamma Z}(q^2)}{q^2 - M_Z^2}\right)\,.$$

The fermion loop contributions to $\Sigma^{\gamma Z}$ vanish at $q^2 = 0$; only the non-Abelian bosonic loops yield $\Sigma^{\gamma Z}(0) \neq 0$.

To be more precise, the charge renormalization as discussed above, is a condition only for the vector coupling constant of the photon. The axial coupling vanishes for on-shell photons as a consequence of the Ward identity.

From the diagonal photon self-energy

$$\Sigma^\gamma(q^2) = q^2\,\Pi^\gamma(q^2)$$

no mass term arises for the photon since, besides the fermion loops, also the bosonic loops behave like

$$\Sigma^{\gamma}_{bos}(q^2) \simeq q^2\,\Pi^{\gamma}_{bos}(0) \to 0$$

for $q^2 \to 0$ leaving the pole at $q^2 = 0$ in the propagator. The absence of mass terms for the photon in all orders is a consequence of the unbroken electromagnetic gauge invariance.

Concluding this discussion we summarize the principal structure of electroweak 1-loop calculations:

- The classical Lagrangian $\mathcal{L}(e, M_W, M_Z, \ldots)$ is sufficent for lowest order calculations and the parameters can be identified with the physical parameters.
- For higher order calculations, $\mathcal{L}$ has to be considered as the "bare" Lagrangian of the theory $\mathcal{L}(e_0, M^0_W, M^0_Z, \ldots)$ with "bare" parameters which are related to the physical ones by

  $$e_0 = e + \delta e, \quad M^{0\,2}_W = M^2_W + \delta M^2_W, \quad M^{0\,2}_Z = M^2_Z + \delta M^2_Z\,.$$

  The counter terms are fixed in terms of a certain subset of 1-loop diagrams by specifying the definition of the physical parameters.
- For any 4-fermion process we can write down the 1-loop matrix element with the bare parameters and the loop diagrams for this process. Together with the counter terms the matrix element is finite when expressed in terms of the physical parameters, i.e. all UV singularities are removed.

4 The vector boson masses

4.1 One-loop corrections to the muon lifetime

The interdependence between the gauge boson masses is established through the accurately measured muon lifetime or the Fermi coupling constant G_μ, respectively. Originally, the μ-lifetime τ_μ has been calculated within the framework of the effective 4-point Fermi interaction. If QED corrections are included one obtains the result [39]

$$\frac{1}{\tau_\mu} = \frac{G^2_\mu m^5_\mu}{192\pi^3}\left(1 - \frac{8m^2_e}{m^2_\mu}\right)\left[1 + \frac{\alpha}{2\pi}(\frac{25}{4} - \pi^2)\right]\,. \tag{48}$$

The leading $2nd$ order correction is obtained by replacing

$$\alpha \to \alpha \left(1 + \frac{2\alpha}{3\pi} \log \frac{m_\mu}{m_e}\right) .$$

This formula is used as the defining equation for G_μ in terms of the experimental μ-lifetime. In lowest order, the Fermi constant is given by the Standard Model expression (26) for the decay amplitude. In 1-loop order, $G_\mu/\sqrt{2}$ coincides with the expression

$$\frac{G_\mu}{\sqrt{2}} \;=\; \frac{e_0^2}{8 s_W^{0\,2} M_W^{0\,2}} \left[1 + \frac{\Sigma^W(0)}{M_W^2} + (vertex, box)\right] . \tag{49}$$

This equation contains the bare parameters with the bare mixing angle

$$s_W^{0\,2} = 1 - \frac{M_W^{0\,2}}{M_Z^{0\,2}} . \tag{50}$$

The term $(vertex, box)$ schematically summarizes the vertex corrections and box diagrams in the decay amplitude. A set of infra-red divergent "QED correction" graphs has been removed from this class of diagrams. These left-out diagrams, together with the real bremsstrahlung contributions, reproduce the QED correction factor of the Fermi model result in Eq. (48) and therefore have no influence on the relation between G_μ and the Standard Model parameters.

Next we evaluate Eq. (49) to 1-loop order by expanding the bare parameters

$$\begin{aligned}
e_0^2 &= (e + \delta e)^2 \;=\; e^2 (1 + 2\frac{\delta e}{e}), \\
M_W^{0\,2} &= M_W^2 \,(1 + \frac{\delta M_W^2}{M_W^2}), \\
s_W^{0\,2} &= 1 - \frac{M_W^2 + \delta M_W^2}{M_Z^2 + \delta M_Z^2} \;=\; s_W^2 + c_W^2 \left(\frac{\delta M_Z^2}{M_Z^2} - \frac{\delta M_W^2}{M_W^2}\right)
\end{aligned} \tag{51}$$

and keeping only terms of 1-loop order:

$$\begin{aligned}
\frac{G_\mu}{\sqrt{2}} &= \frac{e^2}{8 s_W^2 M_W^2} \cdot \\
&\quad \cdot \left[1 + 2\frac{\delta e}{e} - \frac{c_W^2}{s_W^2}\left(\frac{\delta M_Z^2}{M_Z^2} - \frac{\delta M_W^2}{M_W^2}\right) + \frac{\Sigma^W(0) - \delta M_W^2}{M_W^2} + (vertex,\, box)\right] \\
&\equiv \frac{e^2}{8 s_W^2 M_W^2} \cdot [1 + \Delta r]
\end{aligned} \tag{52}$$

which is the 1-loop corrected version of Eq. (26).

The quantity $\Delta r(e, M_W, M_Z, M_H, m_t)$ is the finite combination of loop diagrams and counterterms in Eq. (52). Since we have already determined the counterterms in the previous subsection in terms of the boson self-energies, it is now only a technical problem to evaluate the 1-loop diagrams for the final explicit expression of Δr. Here we quote the result:

$$(vertex,\, box) = \frac{\alpha}{\pi s_W^2}\left(\Delta - \log\frac{M_W^2}{\mu^2}\right) + \frac{\alpha}{4\pi s_W^2}\left(6 + \frac{7-4s_W^2}{2s_W^2}\log c_W^2\right)\,. \quad (53)$$

Therein, the expression

$$\Delta = \frac{2}{\epsilon} - \gamma + \log 4\pi, \quad \epsilon = 4 - D\,, \quad (54)$$

and the mass scale μ are the conventional UV parameters in dimensional regularization. The singular part of Eq. (53), up to a factor, coincides with the non-Abelian bosonic contribution to the charge counterterm in Eq. (47):

$$\frac{\alpha}{\pi s_W^2}\left(\Delta - \log\frac{M_W^2}{\mu^2}\right) \;=\; \frac{2}{c_W\, s_W}\,\frac{\Sigma^{\gamma Z}(0)}{M_Z^2}\,.$$

Together with Eq. (47) and (53) we obtain from Eq. (52):

$$\begin{aligned}\Delta r \;&=\; \Pi^\gamma(0) - \frac{c_W^2}{s_W^2}\left(\frac{\delta M_Z^2}{M_Z^2} - \frac{\delta M_W^2}{M_W^2}\right) + \frac{\Sigma^W(0) - \delta M_W^2}{M_W^2} \\ &\quad +2\,\frac{c_W}{s_W}\,\frac{\Sigma^{\gamma Z}(0)}{M_Z^2} \;+\; \frac{\alpha}{4\pi s_W^2}\left(6 + \frac{7-4s_W^2}{2s_W^2}\log c_W^2\right)\,. \qquad (55)\end{aligned}$$

The first line is of particular interest: via $\Sigma^W(0)$ and the mass counter terms $\delta M_{W,Z}^2$ also the masses M_H, m_t enter Δr, whereas the residual terms depend only on the vector boson masses. We proceed with a more explicit discussion of the gauge invariant subset of fermion loop corrections which involves, among others, the top quark. This subset is also of primordial practical interest since it constitutes the numerically dominating part of Δr.

4.2 Fermion contributions to Δr

In the fermionic vacuum polarization of Eq. (55) we split off the subtracted part evaluated at M_Z^2:

$$\begin{aligned}\Pi^\gamma(0) \;&=\; -\mathrm{Re}\Pi^\gamma(M_Z^2) + \Pi^\gamma(0) + \mathrm{Re}\,\Pi^\gamma(M_Z^2) \\ &=\; -\mathrm{Re}\,\hat{\Pi}^\gamma(M_Z^2) + \mathrm{Re}\,\Pi^\gamma(M_Z^2)\,. \qquad (56)\end{aligned}$$

The subtracted finite quantity $\hat{\Pi}^\gamma(M_Z^2)$ can be split into a leptonic and a hadronic part:

$$\mathrm{Re}\,\hat{\Pi}^\gamma(M_Z^2) = \mathrm{Re}\,\hat{\Pi}^\gamma_{lept}(M_Z^2) + \mathrm{Re}\,\hat{\Pi}^\gamma_{had}(M_Z^2)\,.$$

Heavy fermions decouple; the top quark yields a small contribution

$$\hat{\Pi}^\gamma_{top}(M_Z^2) = \frac{\alpha}{\pi}\,Q_t^2\,\frac{M_Z^2}{5\,m_t^2}\,. \tag{57}$$

Whereas the leptonic content can easily be obtained from

$$\mathrm{Re}\,\hat{\Pi}^\gamma_{lept}(M_Z^2) = \sum_{l=e,\mu,\tau} \frac{\alpha}{3\pi}\left(\frac{5}{3} - \log\frac{M_Z^2}{m_l^2}\right)\,, \tag{58}$$

no light quark masses are available as reasonable input parameters for the hadronic content. Instead, the 5 flavor contribution to $\hat{\Pi}^\gamma_{had}$ can be derived from experimental data with the help of a dispersion relation

$$\hat{\Pi}^\gamma_{had}(M_Z^2) = \frac{\alpha}{3\pi}\,M_Z^2\int_{4m_\pi^2}^{\infty} ds'\,\frac{R^\gamma(s')}{s'(s'-M_Z^2-i\varepsilon)} \tag{59}$$

with

$$R^\gamma(s) = \frac{\sigma(e^+e^-\to\gamma^*\to hadrons)}{\sigma(e^+e^-\to\gamma^*\to\mu^+\mu^-)}$$

as an experimental quantity up to a scale s_1 and applying perturbative QCD for the tail region above s_1. Using e^+e^- data for the energy range below 40 GeV and perturbative QCD for the high energy tail, the recent updates [40,41] yield

$$\mathrm{Re}\,\hat{\Pi}^\gamma_{had}(M_Z^2) = -0.0280 \pm 0.0007 \tag{60}$$

and thus confirm the the previous value [42] with an improved accuracy. The error is almost completely due to the experimental data. Other determinations [43,44] agree within one standard deviation.

Combining this result with the leptonic part one obtains

$$\mathrm{Re}\,\hat{\Pi}^\gamma(M_Z^2) = -0.0593 \pm 0.0007\,.$$

Besides $\Pi^\gamma(M_Z^2)$ we need the W and Z self-energies. For simplicity we restrict the further discussion to a single family, leptons or quarks, with $m_\pm$, $Q_\pm$, $v_\pm$, $a_\pm$ denoting mass, charge, vector and axial vector coupling of the up(+) and down(-) member. At the end, we perform the sum over the various families. We discuss the light and heavy fermions separately:

- Light fermions:

In the light fermion limit, i.e. neglecting all terms $\sim m_\pm/M_{W,Z}$, the various ingredients of Δr read (in case of quark doublets with an additional factor $N_C = 3$):

$$\begin{aligned}
\frac{\Sigma^W(0)}{M_W^2} &= O\left(\frac{m_\pm^2}{M_W^2}\right) \simeq 0\,, \\
\frac{\delta M_Z^2}{M_Z^2} &= \frac{\alpha}{3\pi}\cdot\frac{v_+^2+a_+^2+v_-^2+a_-^2}{4s_W^2c_W^2}\left(\Delta - \log\frac{M_Z^2}{\mu^2} + \frac{5}{3}\right)\,, \\
\frac{\delta M_W^2}{M_W^2} &= \frac{\alpha}{3\pi}\cdot\frac{1}{4s_W^2}\left(\Delta - \log\frac{M_Z^2}{\mu^2} + \frac{5}{3}\right) - \frac{\alpha}{16\pi s_W^2}\log c_W^2\,,
\end{aligned}$$

together with

$$\mathrm{Re}\,\Pi^\gamma(M_Z^2) \;=\; \frac{\alpha}{3\pi}\,(Q_+^2+Q_-^2)\left(\Delta - \log\frac{M_Z^2}{\mu^2} + \frac{5}{3}\right)\,.$$

Inserting everything into Eq. (55) yields

$$\begin{aligned}
\Delta r \;&=\; -\mathrm{Re}\,\hat\Pi^\gamma(M_Z^2) \\
&\quad + \frac{\alpha}{3\pi}\left(\Delta - \log\frac{M_Z^2}{\mu^2} + \frac{5}{3}\right)\cdot \\
&\quad \cdot\left[Q_+^2+Q_-^2 - \frac{c_W^2}{s_W^2}\left(\frac{v_+^2+a_+^2+v_-^2+a_-^2}{4s_W^2c_W^2} - \frac{1}{4s_W^2}\right) - \frac{1}{4s_W^4}\right] \\
&\quad - \frac{\alpha}{3\pi}\,\frac{c_W^2-s_W^2}{4s_W^2}\,\log c_W^2 \\
&=\; -\mathrm{Re}\,\hat\Pi^\gamma(M_Z^2) - \frac{\alpha}{3\pi}\,\frac{c_W^2-s_W^2}{4s_W^4}\,\log c_W^2 \qquad (61)
\end{aligned}$$

The term in brackets [...] is zero with the coupling constants in Eq. (37). Thus, the main effect from the light fermions comes from the subtracted photon vacuum polarization as the remnant from the renormalization of the electric charge at $q^2 = 0$. For this reason, after summing over all light fermions, we can write

$$\Delta\alpha \equiv -\,\mathrm{Re}\,\hat\Pi^\gamma(M_Z^2) \;=\; 0.0593 \pm 0.0007\,. \qquad (62)$$

- Heavy fermions:

Of special interest is the case of the heavy top quark which contributes a large correction $\sim m_t^2$ to Δr. In order to extract this piece we keep for simplicity only those terms which are either singular or quadratic in the top mass $m_t \equiv m_+$ ($N_C = 3$):

$$\mathrm{Re}\,\Pi^\gamma(M_Z^2) = N_C\,\frac{\alpha}{3\pi}(Q_+^2 + Q_-^2)\left(\Delta - \log\frac{m_t^2}{\mu^2}\right) + \cdots$$

$$\frac{\delta M_Z^2}{M_Z^2} = N_C\,\frac{\alpha}{3\pi}\left\{\frac{v_+^2 + a_+^2 + v_-^2 + a_-^2}{4s_W^2 c_W^2} - \frac{3m_t^2}{8s_W^2 c_W^2 M_Z^2}\right\}\left(\Delta - \log\frac{m_t^2}{\mu^2}\right) + \cdots$$

$$\frac{\delta M_W^2}{M_W^2} = N_C\,\frac{\alpha}{3\pi}\left\{\frac{1}{4s_W^2}\left(\Delta - \log\frac{m_t^2}{\mu^2}\right) - \frac{3m_t^2}{8s_W^2 M_W^2}\left(\Delta - \log\frac{m_t^2}{\mu^2} + \frac{1}{2}\right)\right\} + \cdots$$

$$\frac{\Sigma^W(0)}{M_W^2} = -\,N_C\,\frac{\alpha}{3\pi}\cdot\frac{3m_t^2}{8s_W^2 M_W^2}\left(\Delta - \log\frac{m_t^2}{\mu^2} + \frac{1}{2}\right).$$

Inserting into Eq. (55) we verify that the singular parts cancel and a finite term $\sim m_t^2$ remains:

$$(\Delta r)_{b,t} = -\,\mathrm{Re}\hat{\Pi}_b^\gamma(M_Z^2) - \frac{c_W^2}{s_W^2}\,\Delta\rho + \cdots \tag{63}$$

with the quantity [38]

$$\Delta\rho = \left(\frac{\Sigma^Z(0)}{M_Z^2} - \frac{\Sigma^W(0)}{M_W^2}\right)_{b,t} = N_C\,\frac{\alpha}{16\pi s_W^2 c_W^2}\,\frac{m_t^2}{M_Z^2}. \tag{64}$$

As a result of our discussion, we have got a simple form for Δr in the leading terms which is valid also after including the full non-fermionic contributions:

$$\Delta r = \Delta\alpha - \frac{c_W^2}{s_W^2}\,\Delta\rho + (\Delta r)_{remainder}. \tag{65}$$

$\Delta\alpha$ contains the large logarithmic corrections from the light fermions and $\Delta\rho$ the leading quadratic correction from a large top mass. All other terms are collected in the $(\Delta r)_{remainder}$. It should be noted that the remainder also contains a term logarithmic in the top mass (for which our approximation above was too crude) which is not negligible

$$(\Delta r)_{remainder}^{top} = -\frac{\alpha}{4\pi s_W^2}\left(\frac{c_W^2}{s_W^2} - \frac{1}{3}\right)\log\frac{m_t}{M_Z} + \cdots \tag{66}$$

Also the Higgs boson contribution is part of the remainder. For large M_H, it increases only logarithmically ("screening" of a heavy Higgs [45]):

$$(\Delta r)^{Higgs}_{remainder} \simeq \frac{\alpha}{16\pi s_W^2} \cdot \frac{11}{3} \left(\log \frac{M_H^2}{M_W^2} - \frac{5}{6} \right) . \tag{67}$$

The typical size of $(\Delta r)_{remainder}$ is of the order ~ 0.01.

4.3 Higher order contributions

Since Δr contains two large entries, $\Delta\alpha$ and $\Delta\rho$, a careful investigation of higher order effects is necessary.

(i) Summation of large $\Delta\alpha$ terms:

The replacement of the $\Delta\alpha$-part

$$1 + \Delta\alpha \;\rightarrow\; \frac{1}{1 - \Delta\alpha}$$

of the 1-loop result in Eq. (52) correctly takes into account all orders in the leading logarithmic corrections $(\Delta\alpha)^n$, as can be shown by renormalization group arguments [46] The evolution of the electromagnetic coupling with the scale μ is described by the renormalization group equation

$$\mu \frac{d\alpha}{d\mu} = -\frac{\beta_0}{2\pi} \alpha^2 \tag{68}$$

with the coefficient of the 1-loop β-function in QED

$$\beta_0 = -\frac{4}{3} \sum_{f \neq t} Q_f^2 \, . \tag{69}$$

The solution of the RGE contains the leading logarithms in the resummed form. It corresponds to a resummation of the iterated 1-loop vacuum polarization to all orders. The non-leading QED-terms of next order are numerically not significant. Thus, in a situation where large corrections would be due only to the evolution of the electromagnetic charge between two very different scales set by m_f and M_Z, the resummed form

$$G_\mu = \frac{\pi\alpha}{\sqrt{2} M_W^2 s_W^2} \frac{1}{1 - \Delta r} = \frac{\pi\alpha}{\sqrt{2} M_Z^2 c_W^2 s_W^2} \frac{1}{1 - \Delta r} \tag{70}$$

with Δr in Eq. (65) represents a good approximation to the full result.

(ii) Summation of large $\Delta\rho$ terms:

For the heavy top quark also $\Delta\rho$ is large and the powers $(\Delta\rho)^n$ are not correctly resummed in Eq. (70). A result correct in the leading terms up to $O(\alpha^2)$ is instead given by the independent resummation [47]

$$\frac{1}{1-\Delta r} \to \frac{1}{1-\Delta\alpha} \cdot \frac{1}{1+\frac{c_W^2}{s_W^2}\Delta\overline{\rho}} + (\Delta r)_{remainder} \tag{71}$$

where

$$\Delta\overline{\rho} = 3x_t[1 + x_t\rho^{(2)}(\frac{M_H}{m_t})], \quad x_t = \frac{G_\mu m_t^2}{8\pi^2\sqrt{2}} \tag{72}$$

incorporates the result from 2-loop 1-particle irreducible diagrams. For light Higgs bosons $M_H \ll m_t$, where M_H can be neglected, the coefficient

$$\rho^{(2)} = 19 - 2\pi^2 \tag{73}$$

was first calculated in ref. [48]. The general function $\rho^{(2)}$, valid for all Higgs masses, has been derived in [49]. With the resummed ρ-parameter

$$\rho = \frac{1}{1-\Delta\overline{\rho}} \tag{74}$$

Eq. (71) is compatible with the following form of the $M_W - M_Z$ interdependence

$$G_\mu = \frac{\pi}{\sqrt{2}} \frac{\alpha(M_Z^2)}{M_W^2\left(1-\frac{M_W^2}{\rho M_Z^2}\right)} \cdot [1 + (\Delta r)_{remainder}]$$

with

$$\alpha(M_Z^2) = \frac{\alpha}{1-\Delta\alpha}\,. \tag{75}$$

It is interesting to compare this result with the corresponding lowest order $M_W - M_Z$ correlation in a more general model with a tree level ρ-parameter $\rho_0 \neq 1$: the tree-level ρ_0 enters in the same way as the ρ from a heavy top in the minimal model. The same applies for the quadratic mass terms from other particles like scalars or additional heavy fermions in isodoublets with large mass splittings. Hence, up to the small quantity $(\Delta r)_{remainder}$, they are indistinguishable from an experimental point of view ($\Delta\alpha$ is universal). In the minimal model, however, ρ is calculable in terms of m_t, M_H whereas ρ_0 is an *additional* free parameter.

(iii) QCD corrections:

Virtual gluons contribute to the quark loops in the vector boson self-energies at the 2-loop level. For the light quarks this QCD correction is already contained in the result for the hadronic vacuum polarization from the dispersion integral, Eq. (59). Fermion loops involving the top quark get additional $O(\alpha\alpha_s)$ corrections which have been calculated perturbatively [52]. The dominating term represents the QCD correction to the leading m_t^2 term of the ρ-parameter and can be built in by writing instead of Eq. (72):

$$\Delta\overline{\rho} = 3x_t \cdot [1 + x_t\,\rho^{(2)} + \delta\rho_{QCD}] \tag{76}$$

The QCD term [50,51] reads:

$$\delta\rho_{QCD} = -\frac{\alpha_s(\mu)}{\pi}\,c_1 + \left(\frac{\alpha_s(\mu)}{\pi}\right)^2 c_2(\mu) \tag{77}$$

with

$$c_1 = \frac{2}{3}\left(\frac{\pi^2}{3} + 1\right) = 2.8599 \tag{78}$$

and the recently calculated [51] 3-loop coefficent $c_2(\mu)$, which amounts to

$$c_2 = -14.59 \;\text{ for } \mu = m_t \text{ and 6 flavors} \tag{79}$$

with the on-shell top mass m_t. It reduces the scale dependence of ρ significantly and hence is an important entry to decrease the theoretical uncertainty of the standard model predictions for precision observables. As part of the higher order irreducible contributions to ρ, the QCD correction is resummed together with the electroweak 2-loop irreducible term as indicated in Eq. (71).

Beyond the $G_\mu m_t^2\alpha_s$ approximation through the ρ-parameter, the complete $O(\alpha\alpha_s)$ corrections to the self energies are available from perturbative calculations [52] and by means of dispersion relations [53]. All the higher order terms contribute with the same positive sign to Δr, thus making the top mass dependence of Δr significantly flatter. This is of high importance for the indirect determination of m_t from M_W measurements, which is affected by the order of 10 GeV. Recently, also non-leading terms to Δr of the type

$$\Delta r_{(bt)} = 3x_t \left(\frac{\alpha_s}{\pi}\right)^2 \left(a_1\frac{M_Z^2}{m_t^2} + a_2\frac{M_Z^4}{m_t^4}\right)$$

have been computed [54]. They contribute an extra term of +0.0001 to Δr and thus are within the uncertainty from $\Delta\alpha$.

(iv) Non-leading electroweak higher order terms:

The modification of Eq. (71) by placing $(\Delta r)_{remainder}$ into the denominator

$$\frac{1}{1-\Delta r} \;\rightarrow\; \frac{1}{(1-\Delta\alpha)\cdot(1+\frac{c_W^2}{s_W^2}\Delta\overline{\rho})\;-\;(\Delta r)_{remainder}} \tag{80}$$

correctly incorporates the non-leading higher order terms containing mass singularities of the type $\alpha^2\log(M_Z/m_f)$ [55]

In the meantime, the non-leading higher order electroweak terms of the order $G_\mu^2 m_t^2 M_Z^2$ have been calculated explicitly using the on-shell and the $\overline{MS}$ renormalization schemes [56]. An independent calculaton of the Higgs mass dependence of these 2-loop terms has been perforemd in ref. [57].

4.4 Predictions and experimental data

The correlation of the electroweak parameters, complete at the one-loop level and with the proper incorporation of the leading higher order effects, is given by the following equation:

$$\begin{aligned} M_W^2\left(1-\frac{M_W^2}{M_Z^2}\right) &= \frac{\pi\alpha}{\sqrt{2}G_\mu}\cdot\frac{1}{(1-\Delta\alpha)\cdot(1+\frac{c_W^2}{s_W^2}\Delta\overline{\rho})\;-\;(\Delta r)_{remainder}} \\ &\equiv \frac{\pi\alpha}{\sqrt{2}G_\mu}\cdot\frac{1}{1-\Delta r}\,. \end{aligned} \tag{81}$$

The term Δr in Eq. (81) is an effective quantity beyond the 1-loop order, introduced to obtain the formal analogy to the naively resummed first order result in Eq. (70). $\Delta\overline{\rho}$ includes the 2-loop irreducible electroweak and QCD corrections to the ρ-parameter according to Eq. (76). The correlation (81) allows us to predict a value for the W mass after the other parameters have been specified. The predicted value for M_W for $m_t = 175.6 \pm 5.5$ GeV is given by

$$M_W \;=\; 80.317^{+0.097}_{-0.098} \pm 0.034\ \mathrm{GeV}\,. \tag{82}$$

The central value is for a Higgs mass of 300 GeV, the upper and lower values belong to $M_H = 70$ and 1000 GeV; the second uncertainty corresponds to the experimental top mass error. The present experimental value for the W mass from the combined UA2, CDF and D0 results [7] is

$$M_W^{exp} \;=\; 80.41 \pm 0.09\,\mathrm{GeV}\,, \tag{83}$$

and from LEP 2 [6]:

$$M_W^{exp} \;=\; 80.48 \pm 0.14\,\mathrm{GeV}\;, \tag{84}$$

yielding the average

$$M_W^{exp} \;=\; 80.43 \pm 0.08\,\mathrm{GeV} \tag{85}$$

in good agreement with the standard model prediction (82).

We can define the higher order quantity Δr also as a physical observable by

$$\Delta r \;=\; 1 \;-\; \frac{\pi\alpha}{\sqrt{2}G_\mu}\,\frac{1}{M_W^2\left(1-\frac{M_W^2}{M_Z^2}\right)}\,. \tag{86}$$

Experimentally, it is determined by M_Z and M_W. Theoretically, it can be computed from M_Z, G_μ, α after specifying the masses M_H, m_t by solving Eq. (81). Both electroweak and QCD higher order effects yield a positive shift to Δr and thus diminish the slope of the first order dependence on m_t for large top masses. The effect on Δr coming from the Higgs dependent $\rho^{(2)}$ in Eq. (76) is an additional weakening of the sensitivity to m_t for large Higgs masses.

The theoretical prediction for Δr for various Higgs and top masses is displayed in Figure 1.

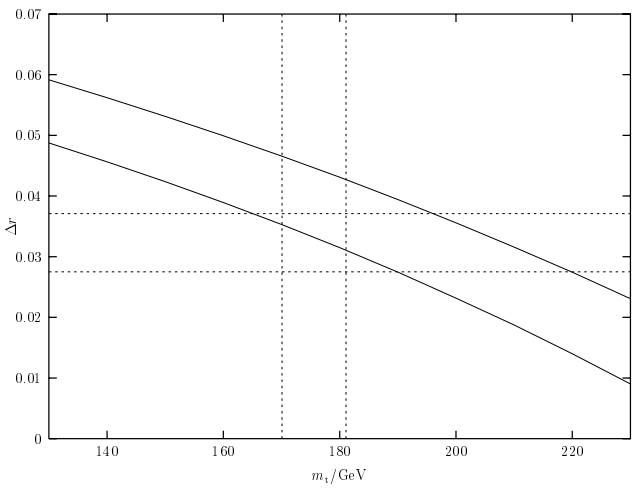

Figure 1: Δr for $M_H = 70$ GeV (lower line) and $M_H = 1$ TeV (upper line), with experimental $\pm 1\sigma$ ranges for m_t and Δr.

For comparison with data, the experimental 1σ limits from the direct measurements of $M_Z = 91.1863$ at LEP [6] and M_W, Eq. (85), are indicated. The constraints on the top mass obtained from these results completely coincide with the direct m_t measurement at the Tevatron of $m_t = 175.6 \pm 5.5$ GeV [8]. The present experimental error does not allow a sensitivity to the Higgs mass. Further precision measurements of M_W at LEP 2 will pin down the error to $\delta\Delta r = 0.0024$ The expected precision in the determination of Δr matches the size of $(\Delta r)_{remainder}$ and thus will provide some sensitivity also to the Higgs mass. For virtual Higgs effects, however, the observables from the Z resonance are more suitable.

4.5 Input from neutrino scattering

The quantity s_W^2 resp. the ratio M_W/M_Z can indirectly be measured in the class of low enery experiments comprising neutrino-quark, neutrino-electron, and electron-quark scattering. The two most precise informations come from the NC/CC neutrino-nucleon cross section ratios [58]. For an isoscalar target these ratios do not depend on the nucleon structure [59]:

$$\begin{aligned} R_\nu &= \frac{\sigma_{NC}^\nu}{\sigma_{CC}^\nu} = \left(\frac{M_W}{M_Z}\right)^4 \frac{1 - 2s_W^2 + \frac{10}{9}(1+r)s_W^4}{2(1-s_W^2)^2} \\ R_{\bar\nu} &= \frac{\sigma_{NC}^{\bar\nu}}{\sigma_{CC}^{\bar\nu}} = \left(\frac{M_W}{M_Z}\right)^4 \frac{1 - 2s_W^2 + \frac{10}{9}(1+\frac{1}{r})s_W^4}{2(1-s_W^2)^2} \end{aligned} \tag{87}$$

with $r = \sigma_{CC}^\nu/\sigma_{CC}^{\bar\nu} \simeq 0.4$.

The second factor in R_ν has a very weak dependence on s_W^2. Hence, measurements of R_ν can directly be converted into values for M_W/M_Z. This principal feature remains valid also after the incorporation of radiative corrections in Eq. (87). Besides the QED corrections, vertex corrections and box diagrams which do not depend on m_t, M_H, the dominant effect $\sim m_t^2$ can simply be embedded in Eq. (87) by replacing

$$s_W^2 \to s_W^2 + c_W^2 \Delta\rho \; .$$

This is obvious from the expansion (51) together with Eq. (64). Since an increase in m_t is equivalent to a slight shift in s_W^2, the relation between R_ν and $(M_W/M_Z)^4$ is affected only marginally. This explains qualitatively the stability of M_W/M_Z against variations of m_t when extracted from R_ν.

The present world average on s_W^2 from the experiments CCFR, CDHS and CHARM [58]

$$s_W^2 = 1 - M_W^2/M_Z^2 = 0.2244 \pm 0.0044 \tag{88}$$

is fully consistent with the direct vector boson mass measurements and with the standard theory.

5 Z physics in electron-positron annihilation

The measurement of the Z mass from the Z line shape at LEP provides us with an additional precise input parameter besides α and G_μ. Other observable quantities from the Z peak, like total and partial decay widths, asymmetries, τ-polarization, allow us to perform precision tests of the theory by comparison with the theoretical predictions.

5.1 Amplitudes and effective couplings

A gauge invariant subset of the 1-loop diagrams to $e^+e^- \to f\bar{f}$ are the QED corrections: The sum of the virtual photon loop graphs is UV finite but IR (= infra-red) divergent because of the massless photon. The IR-divergence is cancelled by adding the cross section with real photon bremsstrahlung (after integrating over the phase space for experimentally invisible photons) which always accompanies a realistic scattering process. Since the phase space for invisible photons is a detector dependent quantity the QED corrections cannot in general be separated from the experimental device.

Our discussion will concentrate on the residual set of 1-loop diagrams, the non-QED or weak corrections. This class is free of IR-singularities but sensitive to the details beyond the lowest order amplitudes. The UV-singular terms associated with the loop diagrams are cancelled by our counterterms of section 3 as a consequence of renormalizability. The 1-loop amplitude for $e^+e^- \to f\bar{f}$ contains the sum of the individual contributions to the self-energies and vertex corrections (including the external fermion self-energies via wave function renormalization). The essential steps for getting the total amplitude finite are: expressing the tree diagrams in terms of the bare parameters e_0, $M_Z^{0\,2}$, $s_W^{0\,2}$ expanding the bare quantities according to Eqs. (44,51), and inserting the counterterms given by Eq. (46) and (47). After some lengthy calculations the total amplitude around the Z pole can be cast into a form close to the lowest order amplitude

$$A(e^+e^- \to f\bar{f}) = A_\gamma + A_Z + (box)$$

as the sum of a dressed photon and a dressed Z exchange amplitude plus the contribution from the box diagrams which are numerically not significant around the peak (relative contribution $< 10^{-4}$). For theoretical consistency (gauge invariance) they have to be retained; for practical purposes they can

be neglected in Z physics. Resummation of the iterated self-energy insertions in the photon and Z propagators brings the finite Z decay width into the denominator, and treats the higher order leading terms in the proper way. Since the leading terms arise from fermion loops only, we do not have problems with gauge invariance; the bosonic loop terms have to be understood as expanded to strict 1-loop order. Numerically their resummation does not yield significant differences but allows a simple and compact notation.

Dressed photon amplitude:

The dressed photon exchange amplitude, with $(p_{e^+} + p_{e^-})^2$,

$$A_\gamma \;=\; \frac{e^2}{1+\hat{\Pi}^\gamma(s)} \cdot \frac{Q_e Q_f}{s} \cdot [(1+F_V^{\gamma e})\gamma_\mu - F_A^{\gamma e}\gamma_\mu\gamma_5] \otimes \Big[(1+F_V^{\gamma f})\gamma^\mu - F_A^{\gamma f}\gamma^\mu\gamma_5\Big] \tag{89}$$

contains $\hat{\Pi}^\gamma$ as the γ self-energy subtracted at $s = 0$. Writing it in the denominator takes into account the resummation of the leading log's from the light fermions, around the Z given by

$$\hat{\Pi}^\gamma_{ferm}(s) = -0.0593 - \frac{40\alpha}{18\pi}\log\frac{s}{M_Z^2} \pm 0.0007 \;+\; i\,\frac{\alpha}{3}\sum_{f\neq t} Q_f^2 N_C^f\,. \tag{90}$$

The form factors $F_{V,A}(s)$ arise from the vertex correction diagrams together with the external fermion self-energies. They vanish for real photons: $F_{V,A}^{\gamma e,f}(0) = 0$. The typical size of the various corrections is (real parts):

$$\begin{aligned} \hat{\Pi}^\gamma(M_Z^2) &= -0.06 \\ F_V^{\gamma e}(M_Z^2) &\simeq F_A^{\gamma e}(M_Z^2) \;\simeq 10^{-3}\,. \end{aligned}$$

For the region around the Z peak, the photon vertex form factors are negligibly small.

Dressed Z amplitude and effective neutral current couplings:

More important is the weak dressing of the Z exchange amplitude. Without the box diagrams the corrections factorize and we obtain a result quite close to the Born amplitude:

$$\begin{aligned} A_Z \;=\; & \sqrt{2}G_\mu M_Z^2(\rho_e\rho_f)^{1/2}\cdot \\ & \cdot\frac{[\gamma_\mu(I_3^e - 2Q_e s_W^2\kappa_e) - I_3^e\gamma_\mu\gamma_5]\otimes[\gamma^\mu(I_3^f - 2Q_f s_W^2\kappa_f) - I_3^f\gamma^\mu\gamma_5]}{s - M_Z^2 \;+\; i\,\frac{s}{M_Z^2}\cdot M_Z\Gamma_Z}\,. \end{aligned} \tag{91}$$

The weak corrections appear in terms of fermion-dependent form factors ρ and κ in the coupling constants and in the width in the denominator.

The s-dependence of the imaginary part is due to the s-dependence of $\mathrm{Im}\Sigma^Z$; the linearization is completely sufficient in the resonance region. We postpone the discussion of the Z width for the moment and continue with the form factors.

The form factors ρ and κ in Eq. (91 have *universal* parts (i.e. independent of the fermion species) and *non-universal* parts which explicitly depend on the type of the external fermions. The universal parts arise from the counterterms and the boson self-energies, the non-universal parts from the vertex corrections and the fermion self-energies in the external lines:

$$\begin{aligned} \rho_{e,f} &= 1 + (\Delta\rho)_{univ} + (\Delta\rho)_{non-univ} \\ \kappa_{e,f} &= 1 + (\Delta\kappa)_{univ} + (\Delta\kappa)_{non-univ}\,. \end{aligned} \tag{92}$$

In their leading terms the universal contributions are given by

$$\begin{aligned} (\Delta\rho)_{univ} &= \Delta\rho + \cdots \\ (\Delta\kappa)_{univ} &= \frac{c_W^2}{s_W^2}\,\Delta\rho + \cdots \end{aligned}$$

with $\Delta\rho$ from Eq. (64). For incorporating the next order leading terms one has to perform the substitutions .

$$\begin{aligned} \rho_{e,f} = 1 + \Delta\rho + \cdots \quad &\to \quad \frac{1}{1-\Delta\overline{\rho}} + \cdots \\ \kappa_{e,f} = 1 + \frac{c_W^2}{s_W}\Delta\rho + \cdots \quad &\to \quad 1 + \frac{c_W^2}{s_W}\Delta\overline{\rho} + \cdots \end{aligned} \tag{93}$$

with $\Delta\overline{\rho}$ from Eq. (76).

The leading structure of the universal parts can easily be understood from the bare amplitude with the counter term expansion

$$\begin{aligned} \frac{e_0^2}{4s_W^{0\,2}c_W^{0\,2}} &= \frac{e^2}{4s_W^2c_W^2}\left[1 + 2\frac{\delta e}{e} - \frac{c_W^2 - s_W^2}{s_W^2}\left(\frac{\delta M_Z^2}{M_Z^2} - \frac{\delta M_W^2}{M_W^2}\right)\right] \\ &= \sqrt{2}G_\mu M_Z^2\left[1 + \frac{\delta M_Z^2}{M_Z^2} - \frac{\delta M_W^2}{M_W^2} + \cdots\right] \end{aligned}$$

and

$$\frac{\delta M_Z^2}{M_Z^2} - \frac{\delta M_W^2}{M_W^2} = \Delta\rho + \cdots$$

in the quadratic m_t-term. Thereby, G_μ was introduced by means of Eq. (52) together with the expression (55) for Δr. In a similar way one finds from Eq. (51):

$$s_W^{0\,2} = s_W^2 \left[1 + \frac{c_W^2}{s_W^2}\left(\frac{\delta M_Z^2}{M_Z^2} - \frac{\delta M_W^2}{M_W^2}\right)\right] = s_W^2 \left[1 + \frac{c_W^2}{s_W^2}\,\Delta\rho + \cdots\right]$$

recovering $(\Delta\kappa)_{univ}$.

The factorized Z amplitude allows us to define NC vertices at the Z resonance with effective coupling constants $g_{V,A}^f$, synonymously to the use of ρ_f, κ_f:

$$\begin{aligned} J_\mu^{NC} &= \left(\sqrt{2} G_\mu M_Z^2 \rho_f\right)^{1/2} \left[(I_3^f - 2Q_f s_W^2 \kappa_f)\gamma_\mu - I_3^f \gamma_\mu\gamma_5\right] \\ &= \left(\sqrt{2} G_\mu M_Z^2\right)^{1/2} \left[g_V^f \gamma_\mu - g_A^f \gamma_\mu\gamma_5\right]. \end{aligned} \tag{94}$$

The complete expressions for the effective couplings read as follows:

$$\begin{aligned} g_V^f &= \left[v_f + 2 s_W c_W\, Q_f \frac{\hat\Pi^{\gamma Z}(M_Z^2)}{1 + \hat\Pi^\gamma(M_Z^2)} + F_V^{Zf}\right] \left(\frac{1 - \Delta r}{1 + \hat\Pi^Z(M_Z^2)}\right)^{1/2}, \\ g_A^f &= \left[a_f + F_A^{Zf}\right] \left(\frac{1 - \Delta r}{1 + \hat\Pi^Z(M_Z^2)}\right)^{1/2}. \end{aligned} \tag{95}$$

Besides Δr, the building blocks, are the following finite combinations of 2-point functions evaluated at $s = M_Z^2$:

$$\begin{aligned} \hat\Pi^Z(s) &= \frac{\mathrm{Re}\,\Sigma^Z(s) - \delta M_Z^2}{s - M_Z^2} - \Pi^\gamma(0) \\ &\quad + \frac{c_W^2 - s_W^2}{s_W^2}\left(\frac{\delta M_Z^2}{M_Z^2} - \frac{\delta M_W^2}{M_W^2} - 2\,\frac{s_W}{c_W}\,\frac{\Sigma^{\gamma Z}(0)}{M_Z^2}\right), \\ \hat\Pi^{\gamma Z}(s) &= \frac{\Sigma^{\gamma Z}(s) - \Sigma^{\gamma Z}(0)}{s} - \frac{c_W}{s_W}\left(\frac{\delta M_Z^2}{M_Z^2} - \frac{\delta M_W^2}{M_W^2}\right) + 2\,\frac{\Sigma^{\gamma Z}(0)}{M_Z^2} \end{aligned} \tag{96}$$

and the finite form factors $F_{V,A}$ at $s = M_Z^2$ from the vertex corrections (includng with the external fermion wave function renormalizations)

$$\begin{aligned} &\Gamma_\mu^{(1-loop)} = \\ &i\,\frac{e}{2 s_W c_W}\left\{\gamma_\mu F_V^{Zf}(s) - \gamma_\mu\gamma_5 F_A^{Zf}(s) + I_3^f \gamma_\mu(1 - \gamma_5)\cdot\frac{c_W}{s_W}\,\frac{\Sigma^{\gamma Z}(0)}{M_Z^2}\right\}, \end{aligned}$$

Due to the imaginary parts of the self energies and vertices, the form factors and the effective couplings, respectively, are complex quantities. The approximation, where the couplings are taken as real, is called the "improved Born approximation".

The Zbb couplings:

The separation of a universal part in the effective couplings is sensible for two reasons: for the light fermions ($f \neq b, t$) the non-universal contributions are small, and (practically) independent of m_t, M_H which enter only the universal part. This is, however, not true for the b-quark where also the non-universal parts have a strong dependence on m_t [60] resulting from the virtual top quark in the vertex corrections. The difference between the d and b couplings can be parametrized in the following way

$$\rho_b = \rho_d (1+\tau)^2, \quad s_b^2 = s_d^2 (1+\tau)^{-1} \tag{97}$$

with the quantity

$$\tau = \Delta\tau^{(1)} + \Delta\tau^{(2)} + \Delta\tau^{(\alpha_s)}$$

calculated perturbatively, at the present level comprising: the complete 1-loop order term [60] with x_t from Eq. (72):

$$\Delta\tau^{(1)} = -2x_t - \frac{G_\mu M_Z^2}{6\pi^2\sqrt{2}}(c_W^2+1)\log\frac{m_t}{M_W} + \cdots, \tag{98}$$

the leading electroweak 2-loop contribution of $O(G_\mu^2 m_t^4)$ [49,61]

$$\Delta\tau^{(2)} = -2\, x_t^2\, \tau^{(2)}, \tag{99}$$

where $\tau^{(2)}$ is a function of M_H/m_t with $\tau^{(2)} = 9 - \pi^2/3$ for $M_H \ll m_t$; the QCD corrections to the leading term of $O(\alpha_s G_\mu m_t^2)$ [62]

$$\Delta\tau^{(\alpha_s)} = 2\, x_t \cdot \frac{\alpha_s}{\pi} \cdot \frac{\pi^2}{3}, \tag{100}$$

and the $O(\alpha_s)$ correction to the $\log m_t/M_W$ term in (98), with a numerically very small coefficient [63].

Effective mixing angles:

Due to the imaginary parts of the self energies and vertices, the form factors and the effective couplings, respectively, are complex quantities. We can define

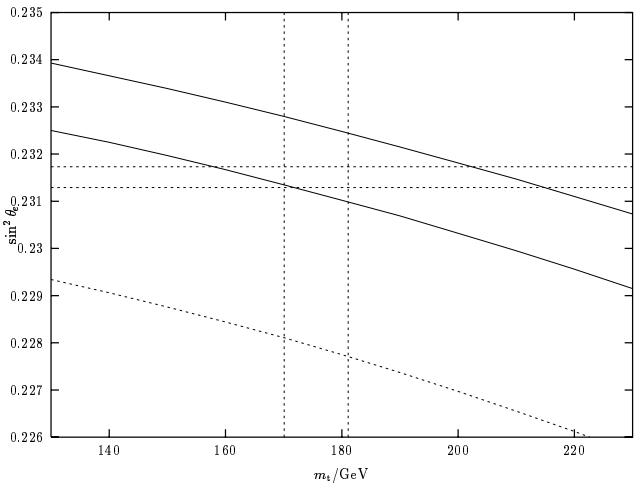

Figure 2: $\sin^2\theta_e$ for $M_H = 70$ GeV (lower line) and $M_H = 1$ TeV (upper line). Also shown are the experimental data ($\pm 1\sigma$ ranges) for m_t and s_e^2 (LEP/SLC average). The dotted curve includes only the fermionic loop effects via $\Delta\alpha$ and $\Delta\rho$.

effective mixing angles according to

$$s_f^2 := \sin^2\theta_f = s_W^2 \,\mathrm{Re}\,\kappa_f = \frac{1}{4 \mid Q_f \mid}\left(1 - \frac{\mathrm{Re}\, g_V^f}{\mathrm{Re}\, g_A^f}\right) . \qquad (101)$$

from the effective coupling constants in (95). They are of particular interest since they determine the on-resonance asymmetries, which will be discussed later in section 5.4. Figure 2 displays the leptonic mixing angle s_e^2 and its compatibility with the data.

5.2 The Z line shape

The integrated cross section $\sigma(s)$ for $e^+e^- \to f\bar{f}$ around the Z resonance with unpolarized beams is obtained from the formulae of the previous section in a straight forward way, expressed in terms of the effective vector and axial vector coupling constants. It is, however, convenient to rewrite $\sigma(s)$ in terms of the Z width and the partial widths Γ_e, Γ_f in order to have a more model independent parametrization. The following form [64,65] includes final state photon radiation

and QCD corrections in case of quark final states: [a]

$$\sigma(s) = \frac{12\pi\Gamma_e\Gamma_f}{\mid s - M_Z^2 + iM_Z\Gamma_Z(s) \mid^2} \left\{ \frac{s}{M_Z^2} + R_f \frac{s - M_Z^2}{M_Z^2} + I_f \frac{\Gamma_Z}{M_Z} + \cdots \right\}$$
$$+ \frac{4\pi\,\alpha(s)^2}{3s} Q_f^2 N_C^f K_{QCD} (1 + \delta_{QED}) \qquad (102)$$

with

$$\Gamma_Z(s) = \Gamma_Z \left\{ \frac{s}{M_Z^2} + \epsilon \frac{s - M_Z^2}{M_Z^2} + \cdots \right\} \qquad (103)$$

and $N_C^f = 1$ for leptons and $= 3$ for quarks. The terms R_f, I_f, ϵ are small quantities calculable in terms of the basic parameters. R_f and I_f describe the γ-Z interference (improved Born approximation)

$$R_f = \frac{2\,Q_e Q_f g_V^e g_V^f}{[(g_V^e)^2 + (g_A^e)^2][(g_V^f)^2 + (g_A^f)^2]} \frac{4\pi\alpha(s)}{\sqrt{2}G_\mu M_Z^2}$$
$$I_f = \frac{2\,Q_e Q_f g_V^e g_V^f}{[(g_V^e)^2 + (g_A^e)^2][(g_V^f)^2 + (g_A^f)^2]} \frac{4\pi\alpha(s)}{\sqrt{2}G_\mu M_Z^2} \cdot \frac{s}{M_Z^2} \mathrm{Im}\,\hat{\Pi}^\gamma\,, \qquad (104)$$

and the last term is the QED background from pure photon exchange with

$$\alpha(s) = \frac{\alpha}{1 + \mathrm{Re}\,\hat{\Pi}^\gamma_{ferm}(s)}$$

and $\hat{\Pi}^\gamma_{ferm}$ from Eq. (90). The small correction

$$\epsilon = \sum_f \epsilon_f, \quad \epsilon_f \simeq \frac{6m_f^2}{M_Z^2} \frac{\Gamma_f}{\Gamma_Z} \frac{(g_A^f)^2}{(g_V^f)^2 + (g_A^f)^2}$$

is due to finite fermion mass effects in the final states. I_f and ϵ have negligible influence on the line shape.

The s-dependent width gives rise to a dislocation of the peak maximum by $\simeq -34$ MeV [66,67] The first term in the expansion (102) is the pure Z resonance. It differs from a Breit-Wigner shape by the s-dependence of the width:

$$\sigma_{res}(s) = \sigma_0 \frac{s\Gamma_Z^2}{(s - M_Z^2)^2 + s^2\Gamma_Z^2/M_Z^2}, \quad \sigma_0 = \frac{12\pi}{M_Z^2} \cdot \frac{\Gamma_e\Gamma_f}{\Gamma_Z^2}\,. \qquad (105)$$

[a] Since initial state photon radiation is treated separately the QED correction factor in Eq. (102) has to be removed in Γ_e.

By means of the substitution [67]

$$s - M_Z^2 + is\Gamma_Z/M_Z = (1 + i\gamma)(s - \hat{M}_Z^2 + i\hat{M}_Z\hat{\Gamma}_Z) \tag{106}$$

with

$$\hat{M}_Z = M_Z(1+\gamma^2)^{-1/2}, \;\; \hat{\Gamma}_Z = \Gamma_Z(1+\gamma^2)^{-1/2}, \;\; \gamma = \frac{\Gamma_Z}{M_Z} \tag{107}$$

a Breit-Wigner resonance shape is recovered:

$$\sigma_{res}(s) = \sigma_0 \, \frac{s\hat{\Gamma}_Z^2}{(s - \hat{M}_Z^2)^2 + \hat{M}_Z^2\hat{\Gamma}_Z^2} \tag{108}$$

Numerically one finds: $\hat{M}_Z - M_Z \simeq -34$ MeV, $\hat{\Gamma}_Z - \Gamma_Z \simeq -1$ MeV. σ_0 is not changed. $\hat{M}_Z$ corresponds to the real part of the S-matrix pole of the Z-resonance [68].

QED corrections:

The observed cross section is the result of convoluting Eq. (102) with the initial state QED corrections consisting of virtual photon and real photon bremsstrahlung contributions:

$$\sigma_{obs}(s) = \int_0^{k_{max}} dk \, H(k) \, \sigma(s(1-k)) \, . \tag{109}$$

k_{max} denotes a cut to the radiated energy. Kinematically it is limited by $1 - 4m_f^2/s$ or $1 - 4m_\pi^2/s$ for hadrons, respectively. For the required accuracy, multi-photon radiation has to be included. The radiator function $H(k)$ with soft-photon resummation and the exact $O(\alpha^2)$ result [69] for initial state QED corrections is given in ref. [64]

From line shape measurements one obtains the parameters M_Z, Γ_Z, σ_0 or the partial widths, respectively. Whereas M_Z is used as a precise input parameter, together with α and G_μ, the width and partial widths allow comparisons with the predictions of the Standard Model to be discussed next.

5.3 Z widths and partial widths

The total Z width Γ_Z can be calculated as the sum over the partial decay widths

$$\Gamma_Z = \sum_f \Gamma_f + \cdots, \quad \Gamma_f = \Gamma(Z \to f\bar{f}) \, , \tag{110}$$

where the ellipses indicate other decay channels which, however, are not significant. The fermionic partial widths, when expressed in terms of the effective coupling constants defined in Eq. (95), read:

$$\begin{aligned}\Gamma_f &= \Gamma_0 \sqrt{1-\frac{4m_f^2}{M_Z^2}}\left[\mid g_V^f \mid^2 \left(1+\frac{2m_f^2}{M_Z^2}\right) + \mid g_A^f \mid^2 \left(1-\frac{4m_f^2}{M_Z^2}\right)\right]\cdot \\ &\quad \cdot(1+\delta_{QED}) + \Delta\Gamma_{QCD}^f \qquad (111)\\ &\simeq \Gamma_0\left[\mid g_V^f \mid^2 + \mid g_A^f \mid^2 \left(1-\frac{6m_f^2}{M_Z^2}\right)\right]\cdot(1+\delta_{QED}) + \Delta\Gamma_{QCD}^f\end{aligned}$$

with

$$\Gamma_0 = N_C^f \frac{\sqrt{2}G_\mu M_Z^3}{12\pi}. \qquad (112)$$

The photonic QED correction

$$\delta_{QED} = Q_f^2 \frac{3\alpha}{4\pi} \qquad (113)$$

is very small, maximum 0.17% for charged leptons.

The factorizable QCD corrections for hadronic final states can be written as follows:

$$\Delta\Gamma_{QCD}^f = \Gamma_0\left[\mid g_V^f \mid^2 + \mid g_A^f \mid^2\right]\cdot K_{QCD} \qquad (114)$$

with [71]

$$K_{QCD} = \frac{\alpha_s}{\pi} + 1.41\left(\frac{\alpha_s}{\pi}\right)^2 - 12.8\left(\frac{\alpha_s}{\pi}\right)^3 - \frac{Q_f^2}{4}\frac{\alpha\alpha_s}{\pi^2} \qquad (115)$$

for the light quarks with $m_q \simeq 0$. The recently obtained non-factorizable part of the 2-loop $O(\alpha\alpha_s)$ QCD corrections [72] yields an extra negtive contribution to the partial widths of

$$\begin{aligned}&-1.24(4)\times 10^{-4}\text{GeV} \quad (u\bar{u})\\ &-1.73(6)\times 10^{-4}\text{GeV} \quad (d\bar{d}),\end{aligned}$$

and -0.59(3) MeV for the total hadronic Z width, respectively.

For b quarks the QCD corrections are different due to finite b mass terms and to top quark dependent 2-loop diagrams for the axial part [73]:

$$\Delta\Gamma_{QCD}^b = \Gamma_0\left[\mid g_V^b \mid^2 + \mid g_A^b \mid^2\right]\cdot K_{QCD}$$

$$+\Gamma_0 \mid g_V^b \mid^2 \cdot \frac{12 m_b^2}{M_Z^2} \left[\frac{\alpha_s}{\pi} + \left(\frac{\alpha_s}{\pi} \right)^2 (6.07 - 2\ell) \right.$$
$$\left. + \left(\frac{\alpha_s}{\pi} \right)^3 (2.38 - 24.29\ell + 0.083\ell^2) \right]$$
$$+\Gamma_0 \mid g_A^b \mid^2 \cdot \frac{6 m_b^2}{M_Z^2} \left[\frac{\alpha_s}{\pi}(2\ell - 1) + \left(\frac{\alpha_s}{\pi} \right)^2 (17.96 + 14.14\ell - 0.083\ell^2) \right]$$
$$+\Gamma_0 \mid g_A^b \mid^2 \cdot \frac{1}{3} \left(\frac{\alpha_s}{\pi} \right)^2 I(M_Z^2/4m_t^2) \qquad (116)$$

with

$$\ell = \log \frac{M_Z^2}{m_b^2}$$

and [74]

$$I(x) \simeq -9.250 + 1.037x + 0.632x^2 + 6 \log(2\sqrt{x}) \,.$$

The finite b-mass terms contribute about +2 MeV to the partial Z width into b quarks. Moreover, the top mass dependent correction at the 2-loop level yields an additional, but negative, contribution which cancels part of the positive and constant correction resulting from $m_b \neq 0$ in $O(\alpha_s)$.

Radiation of secondary fermions through photons from the primary final state fermions can yield another sizeable contribution to the partial Z widths which, however, is compensated by the corresponding virtual contribution through the dressed photon propagator in the final state vertex correction. For this compensation it is essential that the analysis is inclusive enough, i.e. the cut to the invariant mass of the secondary fermions is sufficiently large [75].

In table 1 the Standard Model predictions for the various partial widths and the total width of the Z boson are collected. They include all the electroweak, QED and QCD corrections discussed above. Of particular interest are the following ratios of partial widths

$$R_{had} = \frac{\Gamma_{had}}{\Gamma_e}, \quad R_b = \frac{\Gamma_b}{\Gamma_{had}}, \quad R_c = \frac{\Gamma_c}{\Gamma_{had}}. \qquad (117)$$

M_H	Γ_ν	Γ_e	Γ_u	Γ_d	Γ_b	Γ_{had}	Γ_{tot}	R_{had}
60	167.3	84.06	300.5	383.3	375.9	1743.5	2497.3	20.74
300	167.2	83.95	299.8	382.5	375.2	1740.0	2493.1	20.72
1000	166.9	83.81	299.0	381.7	374.2	1736.0	2488.0	20.71

Table 1: Partial and total Z widths in MeV for $m_t = 175$ GeV and various Higgs masses (in GeV). $\alpha_s = 0.118$. Not listed are the values for $\Gamma_\tau = 0.9977\,\Gamma_e$ and Γ_c (very close to Γ_u).

5.4 Asymmetries

Left-right asymmetry

The left-right asymmetry is defined as the ratio

$$A_{LR} = \frac{\sigma_L - \sigma_R}{\sigma_L + \sigma_R} \tag{118}$$

where $\sigma_{L(R)}$ denotes the integrated cross section for left (right) handed electrons. A_{LR}, in case of lepton universality, is equal to the final state polarization in τ-pair production:

$$A^\tau_{pol} = A_{LR}\,. \tag{119}$$

The on-resonance asymmetry ($s = M_Z^2$) in the improved Born approximation is given by

$$A_{LR}(M_Z^2) = A_e \;+\; \Delta A^I_{LR} \;+\; \Delta A^Q_{LR} \tag{120}$$

where the combination

$$A_e = \frac{2 g_V^e g_A^e}{(g_V^e)^2 + (g_A^e)^2} = \frac{2(1 - 4\sin^2\theta_e)}{1 + (1 - 4\sin^2\theta_e)^2} \tag{121}$$

depends only on the effective mixing angle Eq. (101) for the electron. The small contributions from the interference with the photon exchange

$$\Delta A^I_{LR} \;=\; \frac{2 Q_e Q_f\, g_A^e g_V^f}{({g_V^e}^2 + {g_A^e}^2)\,({g_V^f}^2 + {g_A^f}^2)} \frac{4\pi\alpha(M_Z^2)}{\sqrt{2} G_\mu M_Z^2} \cdot \frac{\Gamma_Z}{M_Z} \cdot \mathrm{Im}\,\hat{\Pi}^\gamma \tag{122}$$

and from the pure photon exchange part

$$\Delta A^Q_{LR} \;=\; -\frac{A_e\, Q_e^2 Q_f^2}{({g_V^e}^2 + {g_A^e}^2)\,({g_V^f}^2 + {g_A^f}^2)} \left(\frac{4\pi\alpha(M_Z^2)}{\sqrt{2} G_\mu M_Z^2}\right)^2 \left(\frac{\Gamma_Z}{M_Z}\right)^2 . \tag{123}$$

f	A_e	ΔA_{LR}^I	ΔA_{LR}^Q
μ	0.1511	0.0002	-0.0009
τ	0.1511	0.0002	-0.0009
c	0.1511	0.0005	-0.0003
b	0.1511	0.0004	-0.0001

Table 2: Contributions to the on-resonance left-right asymmetry for various final state fermions. $\sin^2\theta_e = 0.2314$.

are listed in table 2 for the various final state fermions. Except from lepton final states, they are negligibly small. Mass effects from final fermions practically cancel. The same holds for QCD corrections in the case of quark final states, final state QED corrections, and QED corrections from the interference of initial-final state photon radiation. Initial state QED corrections can be treated in complete analogy to Eq. (109) applied to $\sigma_{L,R}(s)$. Their net effect in the asymmetry is also very small and practically independent of cuts [76,77]. A_{LR} thus represents a unique laboratory for testing the non-QED part of the electroweak theory. Measurements of A_{LR} are essentially measurements of $\sin^2\theta_e$ or of the ratio g_V^e/g_A^e.

Forward-backward asymmetries

The forward-backward asymmetry is defined by

$$A_{FB} = \frac{\sigma_F - \sigma_B}{\sigma_F + \sigma_B} \tag{124}$$

with

$$\sigma_F = \int_{\theta>\pi/2} d\Omega \, \frac{d\sigma}{d\Omega}, \quad \sigma_B = \int_{\theta<\pi/2} d\Omega \, \frac{d\sigma}{d\Omega}. \tag{125}$$

For the on-resonance asymmetry ($s = M_Z^2$) we get in the improved Born ap-

proximation:

$$A_{FB}(M_Z^2) \;=\; \frac{3}{4}\cdot A_e\, A_f \left(1 - 4\mu_f + 6\mu_f \frac{(g_A^f)^2}{(g_V^f)^2 + (g_A^f)^2}\right) \;+\; \Delta A_{FB}^I \;+\; \Delta A_{FB}^Q \,. \tag{126}$$

A_f is defined as

$$A_f \;=\; \frac{2 g_V^f g_A^f}{(g_V^f)^2 + (g_A^f)^2} \;=\; \frac{2(1 - 4 \mid Q_f \mid s_f^2)}{1 + (1 - 4 \mid Q_f \mid s_f^2)^2} \tag{127}$$

with the short-hand notation for the effective mixing angle in Eq. (101):

$$s_f^2 \equiv \sin^2 \theta_f \,.$$

The small contributions $\Delta A_{FB}^{I,Q}$ result from the the interference with the photon exchange

$$\Delta A_{FB}^I \quad = \quad \frac{3}{4} \frac{2 Q_e Q_f \, g_A^e g_A^f}{(g_V^{e\,2} + g_A^{e\,2})\,(g_V^{f\,2} + g_A^{f\,2})} \frac{4\pi\alpha(M_Z^2)}{\sqrt{2} G_\mu M_Z^2} \cdot \frac{\Gamma_Z}{M_Z} \cdot \mathrm{Im}\,\hat{\Pi}^\gamma \tag{128}$$

and from the pure photon exchange part:

$$\Delta A_{FB}^Q \quad = \quad -\frac{3}{4} \frac{A_e A_f \, Q_e^2 Q_f^2}{(g_V^{e\,2} + g_A^{e\,2})\,(g_V^{f\,2} + g_A^{f\,2})} \left(\frac{4\pi\alpha(M_Z^2)}{\sqrt{2} G_\mu M_Z^2}\right)^2 \left(\frac{\Gamma_Z}{M_Z}\right)^2 . \tag{129}$$

The on-resonance asymmetries are essentially determined by the values of the effective mixing angles for e and f entering the product $A_e A_f$. Through $s_{e,f}^2$ also the dependence of the asymmetries on the basic Standard Model parameters m_t, M_H is fixed. The small corrections from finite mass effects, interference and photon exchange can be considered practically independent of the details of the model. For demonstrational purpose we list in table 3 the various terms in the on-resonance asymmetries according to Eq. (126) for a common value of the effective mixing angle $s_e^2 = s_f^2 = 0.2314$.

5.5 Uncertainties of the Standard Model predictions

In order to establish in a significant manner possibly small effects from unknown physics we have to know the uncertainties of our theoretical predictions which have to be confronted with the experiments.

The sources of uncertainties in theoretical predictions are the following:

f	$\frac{3}{4}A_eA_f$	mass correction	ΔA_{FB}^I	ΔA_{FB}^Q
μ	0.0171	$< 10^{-6}$	0.0018	-0.0001
τ	0.0171	$1.3 \cdot 10^{-5}$	0.0018	-0.0001
c	0.0758	$2.5 \cdot 10^{-5}$	0.0011	-0.0002
b	0.1061	$1.5 \cdot 10^{-5}$	0.0004	$-5 \cdot 10^{-5}$

Table 3: On-resonance forward-backward asymmetries for $s_f^2 = 0.2314$.

- the experimental errors of the parameters used as an input. With the choice α, G_μ, and M_Z from LEP we can keep these errors as small as possible. The errors from this source are then determined by δM_Z since the errors of α and G_μ are negligibly small. For any of the mixing angles with s_W^2, s_f^2 one finds

$$\frac{\delta s^2}{s^2} = \frac{2\,c^2}{c^2 - s^2}\,\frac{\delta M_Z}{M_Z} \simeq 2 \cdot 10^{-5}\,. \tag{130}$$

- the uncertainties from quark loop contributions to the radiative corrections . Here, we have to distinguish two cases: the uncertainties from the light quark contributions to $\Delta\alpha$ and the uncertainties from the heavy quark contributions to $\Delta\rho$. In both cases the uncertainties are due to strong interaction effects, which are not sufficiently under control theoretically. The problems are due to:
(i) the QCD parameters. The scale of α_s and the definition and scale of quark masses to be used in the calculation of a particular quantity are quite ambiguous in many cases.
(ii) the bad convergence and/or breakdown of perturbative QCD. In particular at low q^2 and in the resonance regions theoretically poorly known nonperturbative effects are non-negligible.

  The theoretical problems with the hadronic contributions of the 5 known light quarks to $\Delta\alpha$ can be circumvented by using the experimental e^+e^--

annihilation cross-section $\sigma_{tot}(e^+e^- \to \gamma^* \to hadrons)$. The error [40]

$$\delta(\Delta\alpha) = \pm 0.0007$$

is dominated by the large experimental errors in $\sigma_{tot}(e^+e^- \to \gamma^* \to hadrons)$ and can be improved only by more precise measurements of hadron production in e^+e^--annihilation at energies well below M_Z. The present uncertainty leads to an error in the W-mass prediction

$$\frac{\delta M_W}{M_W} = \frac{s_W^2}{c_W^2 - s_W^2} \frac{\delta(\Delta r)}{2(1-\Delta r)}$$

of $\delta M_W = 13$ MeV and $\delta \sin^2\theta = 0.00023$ in the prediction of the various weak mixing parameters s_W^2, s_f^2. This matches with the present experimental precision in the electroweak mixing angle.

- The uncertainties from the QCD contributions, besides the 1.6 MeV in the hadronic Z width from $\delta\alpha_s = 0.003$, can essentially be traced back to those in the top quark loops for the ρ-parameter. They can be combined into the following errors [79], which have improved due to the recently available 3-loop result:

$$\delta(\Delta\rho) \simeq 1.5 \cdot 10^{-4}, \ \delta s_\ell^2 \simeq 0.0001$$

for $m_t = 174$ GeV, and slightly larger for heavier top.

- the uncertainties from omission of higher order effects. The size of unknown higher order contributions can be estimated by different treatments of non-leading terms of higher order in the implementation of radiative corrections in electroweak observables ('options') and by investigations of the scheme dependence. Explicit comparisons between the results of 5 different computer codes based on on-shell and $\overline{MS}$ calculations for the Z resonance observables are documented in the "Electroweak Working Group Report" [80] in ref. [81]. Table 4 shows the uncertainty in a selected set of precision observables. The recently calculated non-leading 2-loop corrections [56] $\sim G_\mu^2 m_t^2 M_Z^2$ for Δr and s_ℓ^2 are not included in table 4. They reduce the uncertainty in M_W and s_ℓ^2 considerably, by about a factor ~ 0.3.

Observable O	$\Delta_c O$	$\Delta_g O$
M_W (GeV)	4.5×10^{-3}	1.6×10^{-2}
Γ_e (MeV)	1.3×10^{-2}	3.1×10^{-2}
Γ_Z (MeV)	0.2	1.4
s_e^2	5.5×10^{-5}	1.4×10^{-4}
s_b^2	5.0×10^{-5}	1.5×10^{-4}
R_{had}	4.0×10^{-3}	9.0×10^{-3}
R_b	6.5×10^{-5}	1.7×10^{-4}
R_c	2.0×10^{-5}	4.5×10^{-5}
σ_0^{had} (nb)	7.0×10^{-3}	8.5×10^{-3}
A_{FB}^l	9.3×10^{-5}	2.2×10^{-4}
A_{FB}^b	3.0×10^{-4}	7.4×10^{-4}
A_{FB}^c	2.3×10^{-4}	5.7×10^{-4}
A_{LR}	4.2×10^{-4}	8.7×10^{-4}

Table 4: Largest half-differences among central values (Δ_c) and among maximal and minimal predictions (Δ_g) for $m_t = 175\,\mathrm{GeV}$, $60\,\mathrm{GeV} < M_H < 1\,\mathrm{TeV}$ (from ref. [80])

observable	exp.	$M_H = 65$ GeV	$M_H = 1$ TeV	Δm_t
M_Z (GeV)	91.1863 ± 0.0019	input	input	
Γ_Z (GeV)	2.4947 ± 0.0026	2.4974	2.4881	± 0.0015
σ_0^{had} (nb)	41.489 ± 0.055	41.476	41.483	± 0.003
$\Gamma_{had}/\Gamma_e = R_h$	20.783 ± 0.029	20.753	20.725	± 0.002
$\Gamma_b/\Gamma_{had} = R_b$	0.2169 ± 0.0009	0.2156	0.2157	± 0.0002
$\Gamma_c/\Gamma_{had} = R_c$	0.1732 ± 0.0048	0.1724	0.1723	± 0.0001
A_b	0.870 ± 0.021	0.9340	0.9350	± 0.0001
ρ_ℓ	1.0039 ± 0.0013	1.0056	1.0036	± 0.0006
s_ℓ^2	0.23153 ± 0.00022	0.23114	0.23264	± 0.0002
M_W (GeV)	80.43 ± 0.08	80.417	80.219	± 0.038

Table 5: Precision observables: experimental results [6] and standard model predictions.

6 Standard model and precision data

6.1 Standard model predictions versus data

In table 5 the Standard Model predictions for Z pole observables and the W mass are put together for a light and a heavy Higgs particle with $m_t = 175$ GeV. The last column is the variation of the prediction according to $\Delta m_t = \pm 6$ GeV. The input value for α_s is chosen as $\alpha_s = 0.118$ according to the present world average [82]. Not included are the uncertainties from $\delta\alpha_s = 0.003$, which amount to 1.6 MeV for the hadronic Z width, 0.038 nb for the hadronic peak cross section, and 0.019 for R_h. The other observables are insensitive to small variations of α_s. The experimental results on the Z observables are from combined LEP and SLD data. ρ_ℓ and s_ℓ^2 are the leptonic neutral current couplings in eq. (94), derived from partial widths and asymmetries under the assumption of lepton universality. The table illustrates the sensitivity of the various quantities to the Higgs mass. The effective mixing angle turns out to be the most sensitive observable, where both the experimental error and the uncertainty from m_t are small compared to the variation with M_H. Since a light Higgs boson goes along with a low value of s_ℓ^2, the strongest upper bound on M_H is from A_{LR} at the SLC [83], whereas LEP data alone allow to accommodate also a relatively heavy Higgs (see figure 3). Further constraints on M_H are to be expected in the future from more precise M_W measurements at LEP 2 and the upgraded Tevatron.

Note that the experimental value for ρ_ℓ exhibits the presence of genuine electroweak corrections by 3 standard deviations. The importance of bosonic corrections is visible in the quantity s_e^2, see Figure 2. Deviations from the Standard Model predictions are observed in the ratio $R_b = \Gamma_b/\Gamma_{had}$, in the quantity A_b, repectively A_{FB}^b for b quarks, and in s_ℓ^2 between LEP and SLD.

The W mass prediction in table 5 is obtained by Eq. (81) from M_Z, G_μ, α and M_H, m_t. The indirect determination of the W mass from the global fit to the LEP1/SLD data [6] (see below)

$$M_W = 80.323 \pm 0.042\,\mathrm{GeV}\,,$$

is slightly lower, but still in agreement with the direct measurement (see table 5).

6.2 Standard model fits

Assuming the validity of the Standard Model a global fit to all electroweak results from LEP, SLD, $p\bar{p}$ and νN constrains the parameters m_t, α_s as follows: [6]

$$m_t = 177 \pm 7^{+16}_{-19}\,\mathrm{GeV}, \quad \alpha_s = 0.121 \pm 0.004 \pm 0.002 \tag{131}$$

with $M_H = 300$ GeV for the central value. The second error is from the variation of M_H between 60 GeV and 1 TeV. The fit results include the uncertainties of the Standard Model calculations.

Due to the accuracy of the data reached in the meantime, global fits with respect to both m_t and M_H as free parameters have become available [85]. The results of ref. [6] based on the most recent (but still preliminary) data are displayed in Figure 4. Without the Tevatron constraint on the top mass, the favored range for m_t is a bit lower than the direct measurement. The reason for this behaviour is the strong impact on the upper limit of m_t from the quantity R_b with its high experimental value.

Together with the top mass as an additional experimental data point, the global fit to all electroweak results from LEP, SLD, M_W, νN and m_t yields the solid contour line in Figure 4. Besides the results for m_t and α_s

$$m_t = 173.3 \pm 5.4\,\mathrm{GeV}, \quad \alpha_s = 0.120 \pm 0.003$$

one obtains for the Higgs mass [6]:

$$M_H = 121^{+119}_{-68}\,\mathrm{GeV}\,.$$

The value of α_s is in very good agreement with the world average [82].

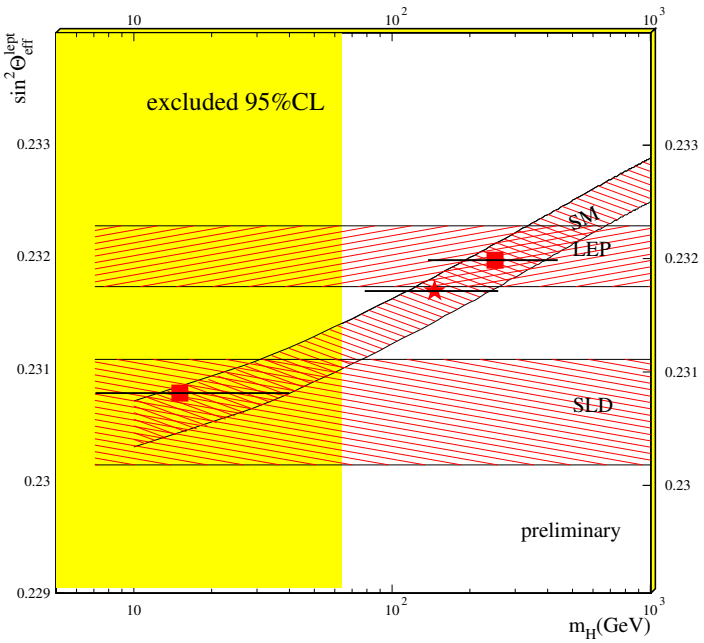

Figure 3: Dependence of the leptonic mixing angle on the Higgs mass. The theoretical predictions correspond to $m_t = 175 \pm 6$ GeV. The SLD and LEP measurements are separately shown. The star is the result of a combined fit to LEP and SLD data, the squares are for separate fits (from ref. [84])

The impact of R_b in this overall fit is not very strong, whereas A_{LR} is decisive for a restrictive upper bound for M_H. Without A_{LR}, the 95% C.L upper bound is shifted upwards by about 260 GeV [84].

The numbers given above do not yet include the theoretical uncertainties of the standard model predictions. The LEP-EWWG [6] has performed a study of the influence of the various 'options' discussed in section 5.5 on the bounds for the Higgs mass with the result that the 95% C.L. upper bound is shifted by nearly 100 GeV to higher values, yielding

$$M_H < 430\,\mathrm{GeV}\,(95\%C.L.)\,.$$

It has to be kept in mind, however, that this error estimate is based on the uncertainties as given in table 1. Since the recent improvement in the theoretical

prediction [56] is going to reduce the theoretical uncertainty especially in the effective mixing angle one may expect also a significant smaller theoretical error on the Higgs mass bounds once the 2-loop terms $\sim G_\mu^2 m_t^2 M_Z^2$ are implemented in the codes used for the fits. At the present stage the codes are without the new terms.

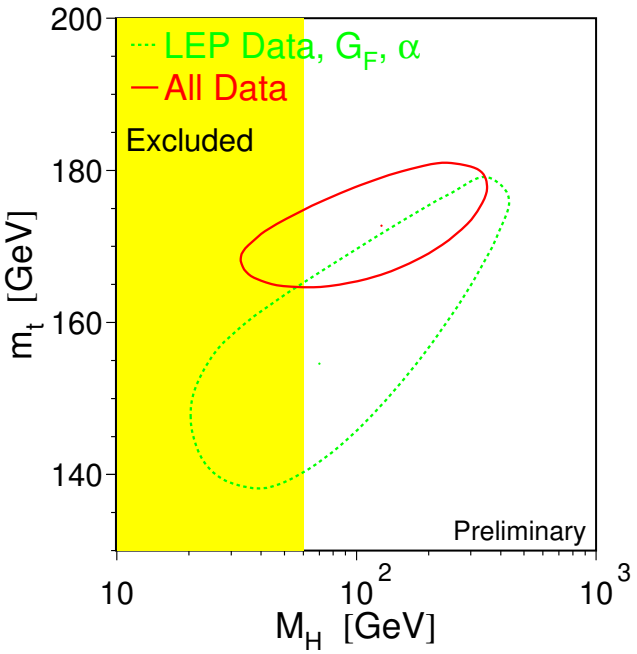

Figure 4: The 68% confidence level contours in the top and Higgs masses for the fits to the LEP data only (dashed) and to all data (solid) including m_t measurements (from ref. [6])

7 Beyond the minimal model

We want to conclude with an outlook on two types of renormalizable generalizations of the minimal model: extensions within SU(2)×U(1) with $\rho_{tree} \neq 1$ and the minimal supersymmetric version of the Standard Model.

7.1 Models with $\rho_{tree} \neq 1$

One of the basic relations of the minimal Standard Model is the tree level correlation between the vector boson masses and the electroweak mixing angle

$$\rho_{tree} = \frac{M_W^2}{M_Z^2 \cos^2 \theta_W} = 1 \,.$$

The formulation of the electroweak theory in terms of a local gauge theory requires at least a single scalar doublet for breaking the electroweak symmetry $\mathrm{SU}(2)\times\mathrm{U}(1) \to \mathrm{U}(1)_{em}$. In contrast to the fermion and vector boson part, very little is known empirically about the scalar sector. Without the assumption of minimality, quite a lot of options are at our disposal, including more complicated multiplets of Higgs fields. The presence of at least a triplet of Higgs fields gives rise to $\rho_{tree} = \rho_0 \neq 1$. As a consequence, the tree level relations between the electroweak parameters have to be generalized according to

$$\sin^2 \theta_W \;\to\; s_\theta^2 = 1 - \frac{M_W^2}{\rho_0 M_Z^2} \tag{132}$$

and

$$\frac{G_\mu}{\sqrt{2}} = \frac{e^2}{8 s_\theta^2 M_W^2} = \frac{e^2}{8 s_\theta^2 c_\theta^2 \rho_0 M_Z^2} \tag{133}$$

A complete discussion of radiative corrections requires the calculation of the extra loop diagrams from the non-standard Higgs sector and an extension of the renormalization procedure [13,86,87]. Since M_W, M_Z and $\sin^2\theta_W$ (or ρ_0, eqivalently) are now independent parameters, one extra renormalization condition is required. A natural condition would be to define the mixing angle for electrons s_e^2 in terms of the ratio of the dressed coupling constants at the Z peak

$$\frac{g_V^e}{g_A^e} =: 1 - 4 s_e^2$$

which is measureable in terms of the left-right or the forward-backward asymmetries. This fixes the counter term for s_e^2 by

$$\frac{\delta s_e^2}{s_e^2} = \frac{c_e}{s_e} \frac{\mathrm{Re}\,\Sigma^{\gamma Z}(M_Z^2)}{M_Z^2} + \frac{c_e}{s_e} \frac{\Sigma^{\gamma Z}(0)}{M_Z^2} + \Delta\kappa_e \tag{134}$$

with the finite part $\Delta\kappa_e$ of the electron-Z vertex correction. The counter terms for the other parameters α, M_Z are treated as usual. With this input,

we obtain a renormalized ρ-parameter and the corresponding counter term for the bare ρ-parameter $\rho_0 = \rho + \delta\rho$ as follows:

$$\begin{aligned} \rho &= \frac{M_W^2}{M_Z^2 c_e^2}\,, \\ \frac{\delta\rho}{\rho} &= \frac{\delta M_W^2}{M_W^2} - \frac{\delta M_Z^2}{M_Z^2} + \frac{\delta s_e^2}{c_e^2}\,. \end{aligned} \tag{135}$$

Other derived quantities are:

- The relation between M_W and G_μ:

$$M_W^2 = \frac{\pi\alpha}{\sqrt{2} G_\mu s_e^2} \cdot \frac{1}{1-\Delta r} \tag{136}$$

with

$$\Delta r = \frac{\Sigma^W(0) - \delta M_W^2}{M_W^2} + \Pi^\gamma(0) - \frac{\delta s_e^2}{s_e^2} + 2\frac{c_e}{s_e}\frac{\Sigma^{\gamma Z}(0)}{M_Z^2} + \delta_{VB} \tag{137}$$

where the vertex-box contribution is given by

$$\delta_{VB} = \frac{\alpha}{4\pi s_e^2}\left(6 + \frac{10 - 10 s_e^2 - 3(1-2s_e^2)\, c_W^2/c_e^2}{2\,(1-c_W^2)} \log c_W^2\right), \quad c_W = \frac{M_W}{M_Z}\,.$$

- The normalization of the Zff couplings at 1-loop:

$$\begin{aligned} &\frac{e^2}{4 s_e^2 c_e^2}\left[1 + \Pi^\gamma(0) - \frac{c_e^2 - s_e^2}{c_e^2}\frac{\delta s_e^2}{s_e^2} + 2\frac{c_e^2 - s_e^2}{c_e s_e}\frac{\Sigma^{\gamma Z}(0)}{M_Z^2} + \Delta\rho_f\right] \\ &= \sqrt{2} G_\mu M_Z^2 \rho\left[1 - \frac{\Sigma^W(0) - \delta M_W^2}{M_W^2} + \frac{\delta s_e^2}{c_e^2} - 2\frac{s_e}{c_e}\frac{\Sigma^{\gamma Z}(0)}{M_Z^2} - \delta_{VB} + \Delta\rho_f\right] \end{aligned} \tag{138}$$

where $\Delta\rho_f$ denotes the finite part of the Zff vertex correction.

- The effective mixing angles of the Zff couplings:

$$s_f^2 = s_e^2\,(1 - \Delta\kappa_e + \Delta\kappa_f).$$

These relations predict the Z boson couplings, M_W and ρ in terms of the data points $\alpha, G_\mu, M_Z, s_e^2$. By this procedure, the m_t^2-dependence of the self energy corrections to theoretical predictions is absorbed into the renormalized ρ-parameter, leaving a $\sim \log m_t/M_Z$ term as an observable effect. For the

Zbb-vertex, an additional m_t^2 dependence is found in the non-universal vertex corrections $\Delta\rho_b$ and $\Delta\kappa_b$. This makes observables containing this vertex the most sensitive top indicators in the class of models with $\rho_{tree} \neq 1$.

Given a specific model, one can calculate the value for ρ from

$$\rho = \frac{\pi\alpha}{\sqrt{2}G_\mu M_Z^2 s_e^2 c_e^2} \cdot \frac{1}{1-\Delta r} \tag{139}$$

in terms of the input data $\alpha, G_\mu, M_Z, s_e^2$ together with m_t and the parameters of the Higgs sector. Such a complete calculation has been performed for a model with an extra Higgs triplet, involving one extra neutral Higgs and a pair of charged Higgs bosons [87]. Figure 5 shows that the model predictions coincide in the area of the experimental data points for m_t and ρ from Eq. (135).

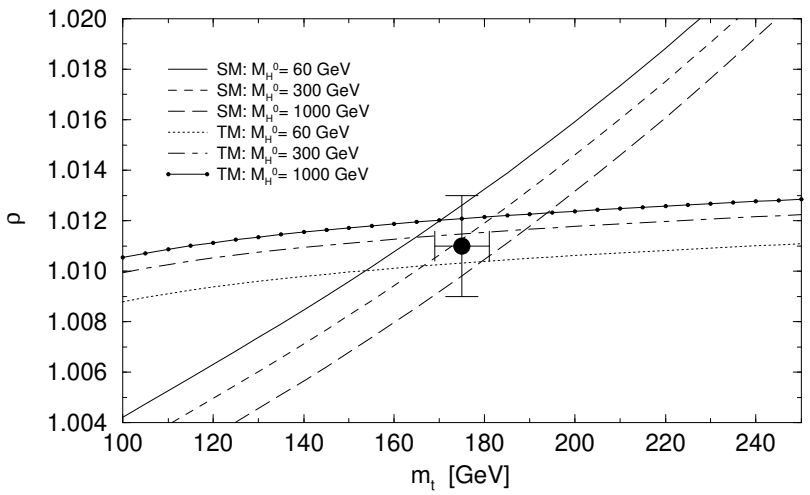

Figure 5: The ρ parameter, Eq. (135), in the Standard Model (SM) and in a model with an extra Higgs triplet (TM). The masses of the non-standard Higgs bosons of TM are set to 300 GeV. $\rho(TM)$ is calculated from Eq. (139) with the LEP input on s_e^2.

7.2 The minimal supersymmetric standard model (MSSM):

The MSSM deserves a special discussion as the most predictive framework beyond the minimal model. Its structure allows a similarly complete calculation of the electroweak precision observables as in the standard model in terms of one Higgs mass (usually taken as M_A) and $\tan\beta = v_2/v_1$, together with the set of SUSY soft breaking parameters fixing the chargino/neutralino and scalar fermion sectors. It has been known since quite some time [88] that light non-standard Higgs bosons as well as light stop and charginos predict larger values for the ratio R_b [89,91] (see figures 6, 7). Complete 1-loop calculations are available for Δr [90] and for the Z boson observables [91]. They contain, besides the standard input, the following entries:

Higgs sector: The scalar sector of the MSSM is completely determined by the value of $\tan\beta = v_2/v_1$ and the pseudoscalar mass M_A, together with the radiative corrections. The latter ones are taken into account in terms of the effective potential approximation with the leading terms $\sim m_t^4$, including the mixing in the scalar top system [92]. In this way, the coupling constants of the various Higgs particles to gauge bosons and fermions can be taken over from [93] substituting only the scalar mixing angle α by the improved effective mixing angle which is obtained from the diagonalization of the scalar mass matrix.

Chargino/Neutralino sector: The chargino (neutralino) masses and the mixing angles in the gaugino couplings are calculated from soft breaking parameters M_1, M_2 and μ in the chargino (neutralino) mass matrix [93]. For practical calculations, the GUT relation $M_1 = 5/3\tan^2\theta_W M_2$ is conventionally assumed.

Sfermion sector: The physical masses of squarks and sleptons are given by the eigenvalues of the 2×2 mass matrix with left (L) and right (R) handed entries. Scalar neutrinos appear only as left-handed mass eigenstates. Since the non-diagonal terms are proportional to m_f, it seems natural to assume unmixed sfermions for the lepton and quark case except for the scalar top sector. For the $\tilde{b}$, $\tilde{t}$ system the physical squark masses $m_{\tilde{b}_L}, m_{\tilde{b}_R}$, $m_{\tilde{t}_2}$ can be used together with the stop mixing angle Φ_t. The simlest case is to assume $m_{\tilde{b}_L} = m_{\tilde{b}_R}$, and $\tilde{u}$, $\tilde{d}$, $\tilde{c}$, $\tilde{s}$ to have masses equal to the $\tilde{b}$ squark mass.

A possible mass splitting between $\tilde{b}_L$-$\tilde{t}_L$ yields a contribution to the ρ-parameter $\rho = 1 + \Delta\rho$ in terms of (left-right mixing neglected)

$$\Delta\rho_{\tilde{b}\tilde{t}} = \frac{3G_\mu}{8\pi^2\sqrt{2}}\left(m^2_{\tilde{b}_L} + m^2_{\tilde{t}_L} - 2\frac{m^2_{\tilde{b}_L} m^2_{\tilde{t}_L}}{m^2_{\tilde{b}_L} - m^2_{\tilde{t}_L}}\log\frac{m^2_{\tilde{b}_L}}{m^2_{\tilde{t}_L}}\right) . \qquad (140)$$

As a universal loop contribution, it enters the quantity Δr and the Z boson couplings through the relations (71) and (93) and is thus significantly constrained by the data on M_W and the leptonic widths. Recently thr 2-loop α_s corrections heve been computed [94] which can amount to 30% of the 1-loop $\Delta\rho_{\bar{b}t}$.

For obtaining the optimized SUSY parameter set a global fit to all the electroweak precision data, including the top mass measurement, has been performed [84] with the new data. The essential features are: The difference between the experimental and the SM value of R_b can now be fully explained by the MSSM. Other quantities are practically unchanged. In total, the χ^2 of the fit is slightly better than in the standard model, but due to the larger numbers of parameters, the probability is about the same as for the Sandard Model. A similar situation occurs for large $\tan\beta$ with light Higgs bosons h^0, A^0 not far above 50 GeV.

In order to obtain the best MSSM fits the electroweak precision data were taken into account together with the error correlations, the measurement of the branching ratio $BR(b \to s\gamma)$ by CLEO [96], and the experimental limits on the masses of non-standard particles from LEP and Tevatron [97,98]. R_b increases with decreasing $\tan\beta$, but the $b \to s\gamma$ rate becomes too small if $\tan\beta$ is near one. With $b \to s\gamma$ included in the fit and a free $\tan\beta$, the preferred value of $\tan\beta$ was either around 1.6 or 34. The values of the strong coupling constant and the top mass are very similar in the MSSM:

$$\alpha_s(M_Z) = 0.116 \pm 0.005$$
$$m_t = 172 \pm 5 \text{ GeV}.$$

These values are for the low $\tan\beta$ scenario. For high $\tan\beta$ only the vlaue for α_s changes to $\alpha_s = 0.119 \pm 0.005$. Both low and hingh $\tan\beta$ values of α_s are in good agreement with the SM value and with the world average 0.118 ± 0.003 [82].

A direct comparison to the Standard Model fit is shown in figure 8 for $\tan\beta = 1.6$; a very similar plot is obtained for $\tan\beta = 34$. The particle spectrum for the best fits suggests that some SUSY particles could be within reach of LEP 2. The χ^2 in the region of the best low $\tan\beta$ fit increases slowly for increasing chargino masses. Within the high $\tan\beta$ scenario both neutral h^0, A^0 bosons are light and have practically the same mass. This scenario can safely be excluded if no Higgs bosons will be found at LEP 2.

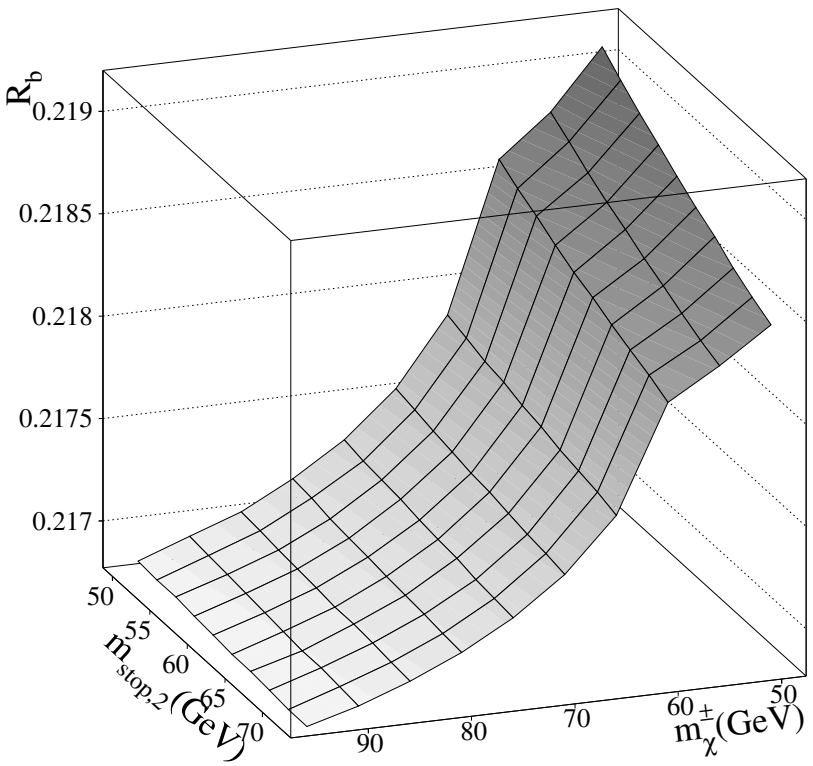

Figure 6: R_b in the light stop-chargino plane. $\tan\beta = 1.6$. [84]

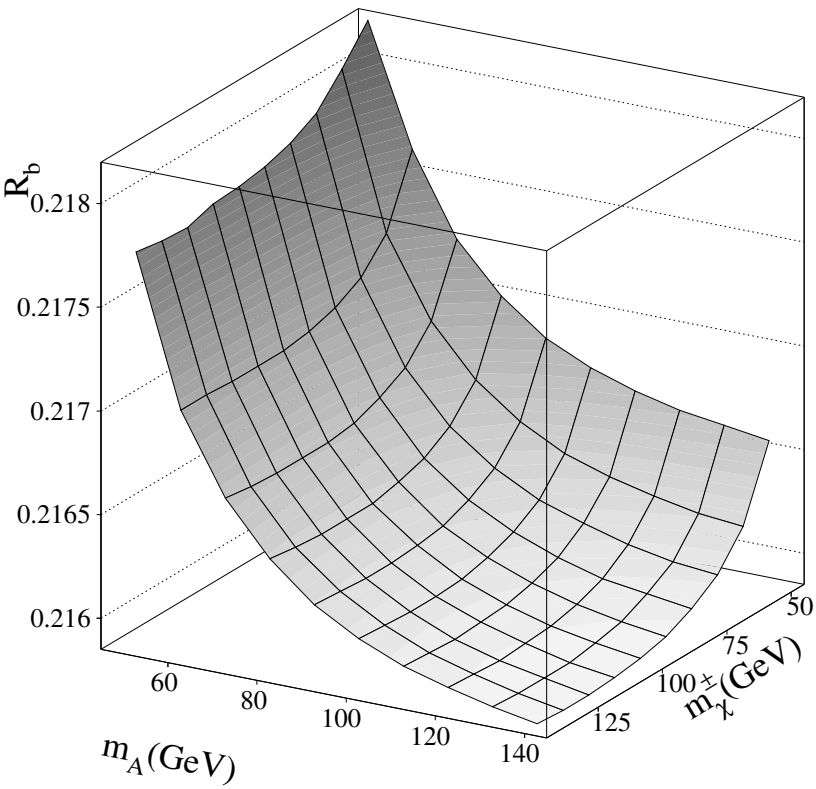

Figure 7: R_b in the pseudoscalar Higgs - chargino plane. $\tan\beta = 34$. [84]

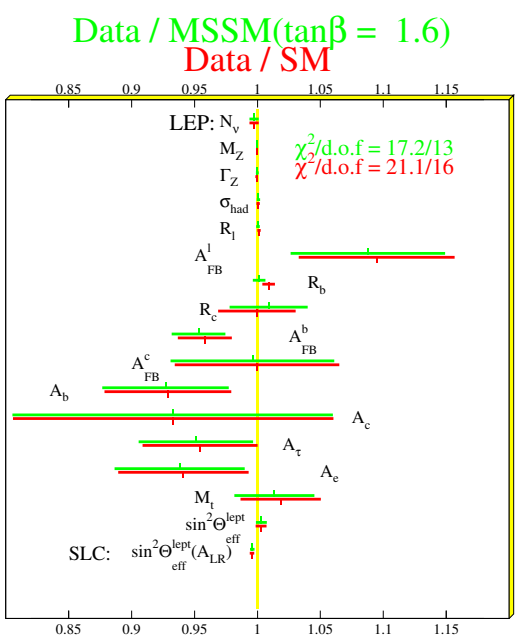

Figure 8: Experimental data normalized to the best fit results in the SM and MSSM, with experimental error bars.

Figure 9 displays the range of predictions for M_W in the minimal model and in the MSSM. Thereby it is assumed that no direct discovery has been at LEP2. As one can see, precise determinations of M_W and m_t can become decisive for the separation between the models.

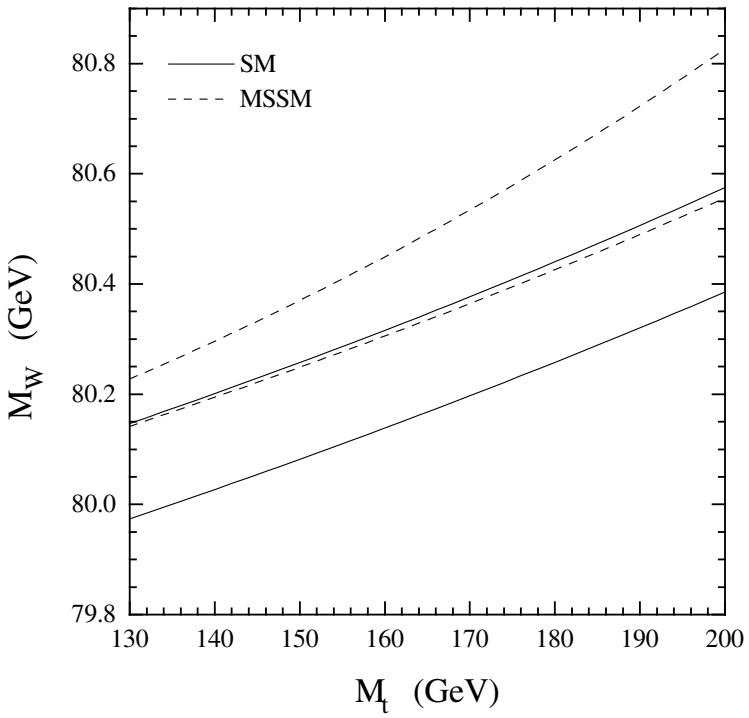

Figure 9: The W mass range in the standard model (—) and the MSSM (- - -). Bounds are from the non-observation of Higgs bosons and SUSY particles at LEP2.

8 Conclusions

Experiments have measured the electroweak observables of the W and Z bosons and the top quark with an impressive accuracy thus providing precision tests of the electroweak theory at a level which had never been reached before. For the interpretation of the precision experiments radiative corrections, better denoted as quantum effects, play a crucial role. The calculation of radiative corrections has been well established over the last years improving and stabilizing the Standard Model predictions. LEP has provided the mass of the Z boson as the third highly accurate input parameter, besides α and G_μ, for completion of the input; each other precision observable provides a test of the electroweak theory. The theoretical predictions of the Standard Model are sensitive to the mass of the meanwhile discovered top quark and to the as yet experimentally unknown Higgs boson through the virtual presence of these particles in the loops. As a consequence, precision data can be used to pin down the allowed range of the mass parameters, yielding m_t in beautiful agreement with the directly measured value. Although the dependence on the Higgs mass is only logarithmic, the experimental precision has reached a level where the sensitivity to M_H becomes visible, with preference for a light Higgs well below the non-perturbative regime. For the future, the reduction of the theoretical uncertainties and more precise data for M_W, m_t and $\sin^2\theta_e$ will be important entries improving the indirect Higgs search.

Theoretical uncertainties in the Standard Model predictions have their origin essentially in the uncertainties of the hadronic vacuum polarization of the photon and from the unknown higher order contributions. In order to reach a theoretical accuracy at the level 0.1% or below, new experimental data on $\Delta\alpha$ and more complete electroweak 2-loop calculations are required. The observed deviations in the quantities R_b, A_b, A_{LR} reduce the quality of the Standard Model fits significantly, but the indirect determination of m_t is remarkably stable. Still impressive is the overall agreement between theory and experiment for the entire set of precision observables. Supersymmetry can even improve the situation slightly due to an enhancement of R_b by new particles in the range around 100 GeV, in particular for a low value of $\tan\beta$. The W mass predicted by the MSSM is always higher than in the Standard Model; from the increasing experimental accuracy for M_W in the future one hence expects an important probe for both the Standard Model and the MSSM.

References

1. S.L. Glashow, *Nucl. Phys.* **B22** (1961) 579;
   S. Weinberg, *Phys. Rev. Lett.* **19** (1967) 1264;
   A. Salam, in: *Proceedings of the 8th Nobel Symposium*, p. 367, ed. N. Svartholm, Almqvist and Wiksell, Stockholm 1968
2. S.L. Glashow, I. Iliopoulos, L. Maiani, *Phys. Rev.* **D2** (1970) 1285;
3. N. Cabibbo, *Phys. Rev. Lett.* **10** (1963) 531;
   M. Kobayashi, K. Maskawa, *Prog. Theor. Phys.* **49** (1973) 652
4. H.Y. Han, Y. Nambu, *Phys. Rev.* **139** (1965) 1006;
   C. Bouchiat, I. Iliopoulos, Ph. Meyer, *Phys. Lett.* **B138** (1972) 652
5. G. 't Hooft, *Nucl. Phys.* **B33** (1971) 173; *Nucl. Phys.* **B35** (1971) 167
6. The LEP Collaborations ALEPH, DELPHI,L3, OPAL, the LEP Electroweak Working Group and the SLD Heavy Flavor Working Group, CERN-PPE/96-183 (1996);
   for the update see: J. Timmermans, talk at the *XVIII International Symposium on Lepton-Photon Interactions*, Hamburg 1997 (to appear in the proceedings)
7. UA2 Collaboration, J. Alitti et al., *Phys. Lett.* **B276** (1992) 354;
   CDF Collaboration, F. Abe et al., *Phys. Rev. Lett.* **65** (1990) 2243; *Phys. Rev.* **D43** (1991) 2070; *Phys. Rev. Lett.* **75** (1995) 11; *Phys. Rev.* **D52** (1995) 4784;
   A. Gordon, talk at the XXXII Rencontre de Moriond, Les Arcs, March 1997 (to appear in the proceedings);
   D0 Collaboration, S. Abachi et al., FERMILAB-PUB-96/177-E;
   Y.Y. Kim, talk at the *XVIII International Symposium on Lepton-Photon Interactions*, Hamburg 1997 (to appear in the proceedings)
8. CDF Collaboration, F. Abe et al., *Phys. Rev. Lett.* **74** (1995) 2626;
   D0 Collaboration, S. Abachi et al., *Phys. Rev. Lett.* **74** (1995) 2632;
   J. Lys (CDF Collaoration), in: Proceedings of the *28th International Conference on High Energy Physics*, Warsaw 1996, eds. Z. Ajduk, A.K. Wroblewski
   S. Protopopescu (D0 Collaboration) in: Proceedings of the *28th International Conference on High Energy Physics*, Warsaw 1996, eds. Z. Ajduk, A.K. Wroblewski
9. L.D. Faddeev, V.N. Popov, *Phys. Lett.* **B25** (1967) 29
10. M. Böhm, W. Hollik, H. Spiesberger, *Fortschr. Phys.* **34** (1986) 687
11. A. Denner, T. Sack, *Nucl. Phys.* **B347** (1990) 203
12. G. Passarino, in: *Proceeedings of the LP-HEP 91 Conference*, Geneva 1991, eds. S. Hegarty, K. Potter, E. Quercigh, World Scientific, Singapore

1992
13. G. Passarino, *Phys. Lett.* **B231** (1989) 458; *Phys. Lett.* **B247** (1990) 587; *Nucl. Phys.* **B361** (1991) 351
14. G. 't Hooft, *Nucl. Phys.* **B61** (1973) 455; *Nucl. Phys.* **B62** (1973) 444
15. D.A. Ross, J.C. Taylor, *Nucl. Phys.* **B51** (1973) 25
16. G. Passarino, M. Veltman, *Nucl. Phys.* **B160** (1979) 151
17. M. Consoli, *Nucl. Phys.* **B160** (1979) 208
18. A. Sirlin, *Phys. Rev.* **D22** (1980) 971;
    W. J. Marciano, A. Sirlin, *Phys. Rev.* **D22** (1980) 2695;
    A. Sirlin, W. J. Marciano, *Nucl. Phys.* **B189** (1981) 442
19. D.Yu. Bardin, P.Ch. Christova, O.M. Fedorenko, *Nucl. Phys.* **B175** (1980) 435; *Nucl. Phys.* **B197** (1982) 1;
    D.Yu. Bardin, M.S. Bilenky, G.V. Mithselmakher, T. Riemann, M. Sachwitz, *Z. Phys.* **C44** (1989) 493
20. J. Fleischer, F. Jegerlehner, *Phys. Rev.* **D23** (1981) 2001
21. K.I. Aoki, Z. Hioki, R. Kawabe, M. Konuma, T. Muta, *Suppl. Prog. Theor. Phys.* **73** (1982) 1;
    Z. Hioki, *Phys. Rev. Lett.* **65** (1990) 683, E:1692; *Z. Phys.* **C49** (1991) 287
22. M. Consoli, S. LoPresti, L. Maiani, *Nucl. Phys.* **B223** (1983) 474
23. D.Yu. Bardin, M.S. Bilenky, G.V. Mithselmakher, T. Riemann, M. Sachwitz, *Z. Phys.* **C44** (1989) 493
24. W. Hollik, *Fortschr. Phys.* **38** (1990) 165
25. M. Consoli, W. Hollik, F. Jegerlehner, in: *Z Physics at LEP 1*, eds. G. Altarelli, R. Kleiss and C. Verzegnassi, CERN 89-08 (1989)
26. G. Passarino, R. Pittau, *Phys. Lett.* **B228** (1989) 89;
    V.A. Novikov, L.B. Okun, M.I. Vysotsky, CERN-TH.6538/92 (1992)
27. M. Veltman, *Phys. Lett.* **B91** (1980) 95;
    M. Green, M. Veltman, *Nucl. Phys.* **B169** (1980) 137, E: *Nucl. Phys.* **B175** (1980) 547;
    F. Antonelli, M. Consoli, G. Corbo, *Phys. Lett.* **B91** (1980) 90;
    F. Antonelli, M. Consoli, G. Corbo, O. Pellegrino, *Nucl. Phys.* **B183** (1981) 195
28. G. Passarino, M. Veltman, *Phys. Lett.* **B237** (1990) 537
29. W.J. Marciano, A. Sirlin, *Phys. Rev. Lett.* **46** (1981) 163;
    A. Sirlin, *Phys. Lett.* **B232** (1989) 123
30. G. Degrassi, S. Fanchiotti, A. Sirlin, *Nucl. Phys.* **B351** (1991) 49
31. G. Degrassi, A. Sirlin, *Nucl. Phys.* **B352** (1991) 342
32. D.C. Kennedy, B.W. Lynn, *Nucl. Phys.* **B322** (1989) 1
33. M. Kuroda, G. Moultaka, D. Schildknecht, *Nucl. Phys.* **B350** (1991) 25

34. J.C. Ward, *Phys. Rev.* **78** (1950) 1824
35. G. 't Hooft, M. Veltman, *Nucl. Phys.* **B135** (1979) 365
36. C. Bollini, J. Giambiagi *Nuovo Cim.* **12B** (1972) 20;
J. Ashmore, *Nuovo Cim. Lett.* **4** (1972) 289;
G. 't Hooft, M. Veltman, *Nucl. Phys.* **B44** (1972) 189
37. P. Breitenlohner, D. Maison, *Comm. Math. Phys.* **52** (1977) 11, 39, 55
38. M. Veltman, *Nucl. Phys.* **B123** (1977) 89;
M.S. Chanowitz, M.A. Furman, I. Hinchliffe, *Phys. Lett.* **B78** (1978) 285
39. R.E Behrends, R.J. Finkelstein, A. Sirlin, *Phys. Rev.* **101** (1956) 866;
T. Kinoshita, A. Sirlin, *Phys. Rev.* **113** (1959) 1652
40. S. Eidelman, F. Jegerlehner, *Z. Phys.* **C67** (1995) 585
41. H. Burkhardt, B. Pietrzyk, *Phys. Lett.* **B356** (1995) 398
42. F. Jegerlehner, *Progress in Particle and Nuclear Physics* **27** (1991) 1, updated from: H. Burkhardt, F. Jegerlehner, G. Penso, C. Verzegnassi, *Z. Phys.* **C43** (1989) 497;
43. M.L. Swartz, *Phys. Rev.* **D53** (1996) 5268
44. A.D. Martin, D. Zeppenfeld, *Phys. Lett.* **B345** (1995) 558
45. M. Veltman, *Acta Phys. Polon.* **B8** (1977) 475.
46. W.J. Marciano, *Phys. Rev.* **D20** (1979) 274
47. M. Consoli, W. Hollik, F. Jegerlehner, *Phys. Lett.* **B227** (1989) 167.
48. J.J. van der Bij, F. Hoogeveen, *Nucl. Phys.* **B283** (1987) 477
49. R. Barbieri, M. Beccaria, P. Ciafaloni, G. Curci, A. Vicere, *Phys. Lett.* **B288** (1992) 95; *Nucl. Phys.* **B409** (1993) 105;
J. Fleischer, F. Jegerlehner, O.V. Tarasov, *Phys. Lett.* **B319** (1993) 249
50. A. Djouadi, C. Verzegnassi, *Phys. Lett.* **B195** (1987) 265
51. L. Avdeev, J. Fleischer, S. M. Mikhailov, O. Tarasov, *Phys. Lett.* **B336** (1994) 560; E: *Phys. Lett.* **B349** (1995) 597;
K.G. Chetyrkin, J.H. Kühn, M. Steinhauser, *Phys. Lett.* **B351** (1995) 331
52. A. Djouadi, *Nuovo Cim.* **100A** (1988) 357;
D. Yu. Bardin, A.V. Chizhov, Dubna preprint E2-89-525 (1989);
B.A. Kniehl, *Nucl. Phys.* **B347** (1990) 86;
F. Halzen, B.A. Kniehl, *Nucl. Phys.* **B353** (1991) 567;
A. Djouadi, P. Gambino, *Phys. Rev.* **D49** (1994) 3499
53. B.A. Kniehl, J.H. Kühn, R.G. Stuart, *Phys. Lett.* **B214** (1988) 621;
B.A. Kniehl, A. Sirlin, *Nucl. Phys.* **B371** (1992) 141; *Phys. Rev.* **D47** (1993) 883;
S. Fanchiotti, B.A. Kniehl, A. Sirlin, *Phys. Rev.* **D48** (1993) 307
54. K.G. Chetyrkin, J.H. Kühn, M. Steinhauser, *Phys. Rev. Lett.* **75** (1995) 3394

55. A. Sirlin, *Phys. Rev.* **D29** (1984) 89
56. G. Degrassi, P. Gambino, A. Vicini, *Phys. Lett.* **B383** (1996) 219;
G. Degrassi, P. Gambino, A. Sirlin, *Phys. Lett.* **B394** (1997) 188
57. S. Bauberger, G. Weiglein, *Nucl. Instrum. Meth.* **A389** (1997) 318; hep-ph/9707510
58. G.L. Fogli and D. Haidt, *Z. Phys.* **C40** (1988) 379;
CDHS Collaboration, H. Abramowicz et al., *Phys. Rev. Lett.* **B57** (1986) 298; A. Blondel et al, *Z. Phys.* **C45** (1990) 361;
CHARM Collaboration, J.V. Allaby et al., *Phys. Lett.* **B177** (1987) 446; *Z. Phys.* **C36** (1987) 611;
CHARM-II Collaboration, D. Geiregat et al., *Phys. Lett.* **B247** (1990) 131;
Phys. Lett. **B259** (1991) 499;
CCFR Collaboration, C.G. Arroyo et al., *Phys. Rev. Lett.* **72** (1994) 3452;
K. McFarlane (CCFR Collaboration), in: Proceedings of the *28th International Conference on High Energy Physics*, Warsaw 1996, eds. Z. Ajduk, A.K. Wroblewski
59. C.H. Llewellyn Smith, *Nucl. Phys.* **B228** (1983) 205
60. A.A. Akhundov, D. Bardin, T. Riemann, *Nucl. Phys.* **B276** (1986) 1;
W. Beenakker, W. Hollik, *Z. Phys.* **C40** (1988) 141;
J. Bernabeu, A. Pich, A. Santamaria, *Phys. Lett.* **B200** (1988) 569; *Nucl. Phys.* **B363** (1991) 326
61. A. Denner, W. Hollik, B. Lampe, *Z. Phys.* **C60** (1993) 93
62. J. Fleischer, O.V. Tarasov, F. Jegerlehner, P. Rączka, *Phys. Lett.* **B293** (1992) 437;
G. Buchalla, A.J. Buras, *Nucl. Phys.* **B398** (1993) 285;
G. Degrassi, *Nucl. Phys.* **B407** (1993) 271;
K.G. Chetyrkin, A. Kwiatkowski, M. Steinhauser, *Mod. Phys. Lett.* **A8** (1993) 2785
63. A. Kwiatkowski, M. Steinhauser, *Phys. Lett.* **B344** (1995) 359;
S. Peris, A. Santamaria, *Nucl. Phys.* **B445** (1995) 252
64. F.A. Berends et al., in: *Z Physics at LEP 1*, CERN 89-08 (1989), eds. G. Altarelli, R. Kleiss, C. Verzegnassi, Vol. I, p. 89;
W. Beenakker, F.A. Berends, S.C. van der Marck, *Z. Phys.* **C46** (1990) 687
65. A. Borelli, M. Consoli, L. Maiani, R. Sisto, *Nucl. Phys.* **B333** (1990) 357
66. G. Burgers, F.A. Berends, W. Hollik, W.L. van Neerven, *Phys. Lett.* **B203** (1988) 177

67. D. Yu. Bardin, A. Leike, T. Riemann, M. Sachwitz, *Phys. Lett.* **B206** (1988) 539
68. G. Valencia, S. Willenbrock, *Phys. Lett.* **B 259** (1991) 373;
R.G. Stuart, *Phys. Lett.* **B272** (1991) 353
69. G. Burgers, F.A. Berends, W.L.van Neerven, *Nucl. Phys.* **B297** (1988) 429; E: *Nucl. Phys.* **B304** (1988) 921
70. W. Beenakker, F.A. Berends, S.C. van der Marck, *Z. Phys.* **C46** (1990) 687
71. K.G. Chetyrkin, A.L. Kataev, F.V. Tkachov, *Phys. Lett.* **B85** (1979) 277;
M. Dine, J. Sapirstein, *Phys. Rev. Lett.* **43** (1979) 668;
W. Celmaster, R. Gonsalves, *Phys. Rev. Lett.* **44** (1980) 560;
S.G. Gorishny, A.L. Kataev, S.A. Larin, *Phys. Lett.* **B259** (1991) 144;
L.R. Surguladze, M.A. Samuel, *Phys. Rev. Lett.* **66** (1991) 560;
A. Kataev, *Phys. Lett.* **B287** (1992 209
72. A. Czarnecki, J.H. Kühn, *Phys. Rev. Lett.* **77** (1996) 3955
73. For a review see: K.G. Chetyrkin, J.H. Kühn, A. Kwiatkowski, in [82], p. 175; *Phys. Rep.* **277** (1996) 189
74. J.H. Kühn, B.A. Kniehl, *Phys. Lett.* **B224** (1990) 229;
Nucl. Phys. **B329** (1990) 547
75. A. Hoang, J.H. Kühn, T. Teubner, *Nucl. Phys.* **B455** (1995) 3; **B452** (1995) 173
76. M. Böhm, W. Hollik *Nucl. Phys.* **B204** (1982) 45; *Z. Phys.* **C 23** (1984) 31
77. S. Jadach, J.H. Kühn, R.G. Stuart, Z. Wąs, *Z. Phys.* **C38** (1988) 609;
J.H. Kühn, R.G. Stuart, *Phys. Lett.* **B200** (1988) 360
78. M. Böhm, W. Hollik et al., in: *Z Physics at LEP 1*, CERN 89-08 (1989), eds. G. Altarelli, R. Kleiss, C. Verzegnassi, Vol. I, p. 203;
J.H. Kühn, P.Zerwas et al., in: *Z Physics at LEP 1*, CERN 89-08 (1989), eds. G. Altarelli, R. Kleiss, C. Verzegnassi, Vol. I, p. 267
79. B.A. Kniehl, in [82], p. 299
80. D. Bardin et al., in [82], p. 7
81. *Reports of the Working Group on Precision Calculations for the Z Resonance*, CERN 95-03 (1995), eds. D. Bardin, W. Hollik, G. Passarino
82. M. Schmelling, in: Proceedings of the *28th International Conference on High Energy Physics*, Warsaw 1996, eds. Z. Ajduk, A.K. Wroblewski
83. SLD Collaboration, P. Rowson, talk at the XXXII Rencontre de Moriond, Les Arcs, March 1997 (to appear in the Proceedings)
84. W. de Boer, A. Dabelstein, W. Hollik, W. Mösle, U. Schwickerath, hep-ph/9609209 (to appear in Z. Phys. C)

85. K. Hagiwara, D. Haidt, S. Matsumoto, KEK-TH-512, DESY 96-192, hep-ph/9706331;
J. Ellis, G.L. Fogli, E. Lisi, *Phys. Lett.* **B389** (1996) 321; *Z. Phys.* **C69** (1996) 627;
G. Passarino, *Acta Phys. Polon.* **B28** (1997) 635;
S. Dittmaier, D. Schildknecht, *Phys. Lett.* **B391** (1997) 420;
S. Dittmaier, D. Schildknecht, G. Weiglein, *Phys. Lett.* **B386** (1996) 247;
P. Chankowski, S. Pokorski, *Acta Phys. Polon.* **27** (1996) 1719
86. B.W. Lynn, E. Nardi, *Nucl. Phys.* **B381** (1992) 467
87. T. Blank, W. Hollik, Karlsruhe preprint KA-TP-3-1997, hep-ph/9703392
88. A. Denner, R. Guth, W. Hollik, J.H. Kühn, *Z. Phys.* **C51** (1991) 695;
J. Rosiek, *Phys. Lett.* **B252** (1990) 135;
M. Boulware, D. Finnell, *Phys. Rev.* **D44** (1991) 2054
89. G. Altarelli, R. Barbieri, F. Caravaglios, *Phys. Lett.* **B314** (1993) 357;
C.S. Lee, B.Q. Hu, J.H. Yang, Z.Y. Fang, J. Phys. G **19** (1993) 13;
Q. Hu, J.M. Yang, C.S. Li, Comm. Theor. Phys. **20** (1993) 213;
J.D. Wells, C. Kolda, G.L. Kane, *Phys. Lett.* **B338** (1994) 219;
G.L. Kane, R.G. Stuart, J.D. Wells, *Phys. Lett.* **B354** (1995) 350;
M. Drees et al., *Phys. Rev.* **B54** (1996) 5598
90. P. Chankowski, A. Dabelstein, W. Hollik, W. Mösle, S. Pokorski, J. Rosiek, *Nucl. Phys.* **B417** (1994) 101;
D. Garcia, J. Solà, Mod. Phys. Lett. A **9** (1994) 211
91. D. Garcia, R. Jiménez, J. Solà, *Phys. Lett.* **B347** (1995) 309; **B347** (1995) 321; D. Garcia, J. Solà, *Phys. Lett.* **B357** (1995) 349;
A. Dabelstein, W. Hollik, W. Mösle, in *Perspectives for Electroweak Interactions in e^+e^- Collisions*, Ringberg Castle 1995, Ed. B.A. Kniehl, World Scientific 1995 (p. 345);
P. Chankowski, S. Pokorski, *Nucl. Phys.* **B475** (1996) 3
92. J. Ellis, G. Ridolfi and F. Zwirner, *Phys. Lett.* **B257** (1991) 83
93. H. P. Nilles, *Phys. Rep.* **110** (1984) 1;
H. E. Haber and G. Kane, *Phys. Rep.* **117** (1985) 75;
J. F. Gunion and H. E. Haber, *Nucl. Phys.* **B272** (1986) 1;
Nucl. Phys. **B402** (1993) 567;
J. F. Gunion, H. E. Haber, G. Kane and S. Dawson: *The Higgs Hunter's Guide,* Addison-Wesley 1990.
94. A. Djouadi, P. Gambino, S. Heinemeyer, W. Hollik, C. Jünger, G. Weiglein, *Phys. Rev. Lett.* **78** (1997) 3626
95. R. Barbieri, G. Gamberini, G. Giudice, G.Ridolfi, *Nucl. Phys.* **B296** (1988) 75

96. CLEO-Collaboration, R. Ammar et al., *Phys. Rev. Lett.* **74** (1995) 2885
97. ALEPH Collaboration, CERN-PPE/96-10;
OPAL Collaboration, CERN-PPE/96-019; CERN-PPE/96-020; DELPHI Collaboration, CERN-PPE/96-75;
D0 Collaboration, *Phys. Rev. Lett.* **76**(1996) 2222;
FERMILAB-PUB-95/380-E;
ALEPH Collaboration, CERN PPE/96-079
98. Particle Data Group, R.M. Barnett et al., *Phys. Rev.* **D54** (1996) 1